Fisheries New Zealand
Tini a Tangaroa

Acoustic estimates of southern blue whiting from the Campbell Island Rise, August-September 2019 (TAN1905)

New Zealand Fisheries Assessment Report 2020/26

Y. Ladroit,
R. L. O'Driscoll,
K. Large

ISSN 1179-5352 (online)
ISBN 978-1-99-002597-6 (online)

September 2020

New Zealand Government

Requests for further copies should be directed to:

Publications Logistics Officer
Ministry for Primary Industries
PO Box 2526
WELLINGTON 6140

Email: brand@mpi.govt.nz
Telephone: 0800 00 83 33
Facsimile: 04-894 0300

This publication is also available on the Ministry for Primary Industries websites at:
http://www.mpi.govt.nz/news-and-resources/publications
http://fs.fish.govt.nz go to Document library/Research reports

TABLE OF CONTENTS

EXECUTIVE SUMMARY

Ladroit, Y.; O'Driscoll, R.L.; Large, K. (2020). Acoustic estimates of southern blue whiting from the Campbell Island Rise, August-September 2019 (TAN1905).

***New Zealand Fisheries Assessment Report 2020/26.* 56 p.**

The 13th acoustic survey of southern blue whiting (SBW) on the Campbell Island Rise took place from 28 August to 25 September 2019 aboard RV *Tangaroa* (TAN1905). Two acoustic snapshots were successfully completed: the first from 3–11 September; the second from 11–21 September. Fifteen bottom trawls were carried out to inform the species composition of acoustic marks, as well as to get the length frequency and spawning state of SBW. There were also two deployments of NIWA's acoustic optical system (AOS).

The first snapshot detected three spawning aggregations in the survey area: a northern aggregation mainly contained in strata 2 and 4; an eastern aggregation mostly in strata 8N, 8S, and 8E; and a southern aggregation entirely in stratum 7S. Stratum boundaries were modified for snapshot 2, based on the fish distribution in snapshot 1 and to optimise the remaining survey time. Little fish movement was observed in the second snapshot, with the eastern aggregation having moved slightly north-west, and the northern aggregation south-east. The commercial fleet mainly fished the northern aggregation. Observer data collected from the commercial fleet showed spawning occurred from 3–18 September (during the survey period), with a second spawning peak from 23–30 September (after the survey).

Immature SBW were mostly distributed on the southern border of stratum 2, western borders of strata 4, 5, and 7N, as well as the north-western corner of stratum 7S, all in the 300–400 m depth range. No juvenile SBW marks were detected in 2019.

The biomass estimate of adult SBW across the whole survey area was 119 175 t (CV 40%) in the first snapshot and 63 115 t (CV 23%) in the second snapshot, resulting in an average estimate of 91 145 t (CV 27%).This is 6% lower than that from the previous survey in 2016 (97 117 t). The biomass estimate for immature SBW was 4060 t (CV 18%), which was similar to that in 2016 (4456 t).

No optically verified measurements of SBW were made using the AOS, so there were no new data to inform estimates of the target strength.

1. INTRODUCTION

Southern blue whiting (*Micromesistius australis*) is one of New Zealand's largest volume fisheries, with annual landings of between 20 000 t and 42 000 t from 2000–17, declining to 16 500 t in 2018, but increasing again to 31 900 t in 2019. Southern blue whiting (SBW) occur in Sub-Antarctic waters, with known spawning grounds on the Bounty Platform, Pukaki Rise, Auckland Islands Shelf, and Campbell Island Rise (Hanchet 1999). The SBW fishery was developed in the early 1970s by the Soviet fleet. Landings have fluctuated considerably, peaking at 76 000 t in the 1991–92 fishing year, when almost 60 000 t were taken from the Bounty Platform stock. SBW was introduced into the QMS from 1 April 2000 with separate TACs for each of the four main stocks in FMA 6. The Campbell Island stock (SBW6I) is the largest of the four southern blue whiting stocks. The TACC for SBW6I was increased to 39 200 t in 2014, but subsequent catches have been below this.

SBW spawning occurs on the Bounty Platform from mid-August to early-September, and three to four weeks later in the other areas. During spawning, SBW typically form large midwater aggregations. Commercial and research fishing on spawning SBW aggregations result in very clean catches of SBW. The occurrence of single-species spawning aggregations allows accurate biomass estimation using acoustics.

A time series of acoustic surveys for SBW on the Campbell Plateau was started in 1993. The acoustic surveys are used to measure relative abundance of adult SBW and to predict pre-recruit numbers into the stock. The movement of fish during the survey period required the development of an adaptive survey design to increase efficiency. There were 12 previous surveys of the Campbell grounds in 1993, 1994, 1995, 1998, 2000, 2002, 2004, 2006, 2009, 2011, 2013, and 2016. Biomass estimates of SBW in the two most recent surveys in 2013 (O'Driscoll et al. 2014) and 2016 (O'Driscoll et al. 2018) were relatively high, following the recruitment of the above-average 2006, 2009, and 2011 year classes into the fishery. Because SBW recruit at 2 and 3 years to the fishery, surveys are currently scheduled every 3 years to keep the assessment up to date.

Knowledge of target strength (TS) of SBW is necessary for converting the backscatter attributed to SBW to an estimate of biomass. The relationship between TS and fork length (FL) for SBW was revised based on *in situ* TS data collected with a towed acoustic-optical system (AOS) during the 2011 Campbell survey (O'Driscoll et al. 2013). This relationship gives TS values that are within 1 dB of those for northern hemisphere blue whiting (*Micromesistius poutassou*) obtained from *in situ* measurements by Pedersen et al. (2011), but that are higher than those previously estimated for SBW based on swimbladder models (Dunford & Macaulay 2006). O'Driscoll et al. (2013) found that the steep slope in the previous model estimates of SBW TS (Dunford & Macaulay 2006) was likely due to an inappropriate application of the Kirchhoff-approximation model at small swimbladder sizes, but noted that further work is required to attempt to reconcile differences between SBW swimbladder modelling and *in situ* TS results.

1.1 Project objectives

This report summarises results obtained during the 13th acoustic survey of SBW on the Campbell Island Rise in August-September 2019 and provides biomass estimates, fulfilling the reporting requirements for Objectives 1 and 2 of Fisheries New Zealand Project SBW2019-01.

The overall objective for this project was to estimate the biomass of SBW on the Campbell Island Rise (SBW6I) using acoustic survey. There were two objectives:

1. To estimate pre-recruit and spawning biomass at Campbell Island using an acoustic survey, with a target coefficient of variation (CV) of the estimate of 30% or less.
2. To collect *in situ* data on tilt-angle distribution and target strength of southern blue whiting and update the length to tilt-averaged target strength relationship, as appropriate.

2. METHODS

2.1 Survey design

The time series of acoustic estimates for the Campbell Island Rise SBW stock are from area-based surveys which provide fishery independent monitoring of the recruited part of the population as well as predicting the strength of year classes about to enter the fishery. Although much of the adult spawning biomass may be concentrated in one or more localised aggregations, an aggregation-based survey design is not appropriate for this fishery, because a variable proportion of the biomass occurs away from these aggregations. The acoustic survey is also used to estimate abundance of pre-recruit SBW, which typically occur outside the area being fished by the commercial fleet. Attempts have been made to survey the main SBW spawning aggregations on the Campbell Island Rise from industry vessels in 2003 (O'Driscoll & Hanchet 2004), 2006 (O'Driscoll et al. 2006), and 2010 (O'Driscoll 2011), but these gave much lower estimates of SBW biomass than those obtained from wide-area surveys. For example, the aggregation-based survey by two industry vessels in 2006 gave estimates of abundance that were only 10–15% of those from the wide-area research survey in the same year (O'Driscoll et al. 2006, 2007).

The most suitable time for an acoustic survey of SBW is when they aggregate to spawn. On the Campbell Island Rise, the onset of spawning over the past 15 years has typically been from 6 to 17 September (range 3–20 September). The 2019 survey was carried out from 28 August to 25 September 2019 to maximise the chances of covering the spawning period. The 29-day booking of *Tangaroa* allowed for 21 days in the survey area, 1 day for acoustic calibration, 2 days for loading and unloading, and 5 days steaming to and from Wellington. Within the 21 days of survey time, allowance was made for 2 days for camera work (Objective 2), and 3 days for bad weather.

The study aimed to carry out at least two snapshots of the Campbell Island Rise spawning area with an overall target CV of 30% (as specified by the project objectives). The survey followed the two-phase design recommended by Dunn & Hanchet (1998) and Dunn et al. (2001), incorporating the modifications recommended by Hanchet et al. (2003).

The survey area extended from the 300 m depth contour in the west to the eastern and southern boundaries of the Campbell Plateau, which varied in depth from about 480 to 750 m. The distribution of historic commercial catch and effort (Figure 1) and the results from previous acoustic surveys were used as a basis for the survey stratification and allocation of transects for snapshot 1 (Table 1, Figure 2). The stratum boundaries for snapshot 1 were the same as those for snapshot 1 of the 2016 survey. Transect locations were randomly generated and were carried out at right angles to the depth contours (i.e., from shallow to deep or vice versa). The minimum distance between transect midpoints varied between strata and was calculated as follows:

$$m = 0.5\,L/n \qquad (1)$$

where m is the minimum spacing distance in nautical miles, L is the length of the stratum in nautical miles, and n is the number of transects.

During snapshot 1, an aggregation was detected on the southernmost transect of stratum 8S, so this stratum was extended 10 nautical miles to the south to 52° 50' S and an extra transect was added (Figure 2). One of the four planned transects in stratum 6N was not completed (Table 1).

Several modifications were made to stratum boundaries for snapshot 2 (Figure 2, Table 2) based on the location of the main fish aggregations observed during snapshot 1 and the location of the commercial fishing fleet (Figure 4). These were:

1. Merging of strata 6N and 6S into a single stratum 62, with its southern boundary being reduced to 52° 45' S;

2. Merging of strata 8E, 8N, and 8S into a single stratum 82, with a southern boundary set at 52° 45’ S and an eastern boundary reduced to 171° 45’ E;
3. Reduction of stratum 7S to 7S2 with its western boundary at 169° 45’ E and southern boundary at 53° 30’ S.

2.2 Acoustic data collection

The survey was undertaken using hull-mounted and towed acoustic systems. The hull-mounted system of five Simrad EK60 echosounders (18, 38, 70, 120, and 200 kHz) was used as long as the weather did not degrade the data acquired (usually in less than 25 knots winds). The towed system was a single-frequency (38 kHz) re-packaged Simrad EK60 mounted in a 3-m long towed body (Towbody 4), which allowed good quality data to be obtained in harsher weather conditions, up to 40 knots winds and 6–7 m swells.

The acoustic equipment used during the survey was calibrated following the procedures given by Demer et al. (2015). The hull system was calibrated on 30 August 2019 in Queen Charlotte Sound soon after departure. The acoustic towbody was also calibrated on 30 August in Queen Charlotte Sound, and again on 17 September in Perseverance Harbour while sheltering from bad weather. Calibration reports for the hull and Towbody 4 systems can be found in Appendices 1 and 2 respectively.

Transects were run at speeds of 6–10 knots (depending on the weather and sea conditions). When the acoustic towbody was used, it was deployed 30–70 m below the surface. There is no evidence to suggest a strong diel variation in SBW backscatter on the Campbell grounds (Hanchet et al. 2000), so transects were carried out during day and night. Acoustic data collection was interrupted between transects for mark identification trawls.

2.3 Trawling

Trawling was carried out for mark identification, biological sampling, and for AOS deployments. As in previous surveys, most demersal marks were targeted using the ratcatcher wing trawl, with 50 m sweeps, 50 m bridles and a 40 mm mesh codend. The hoki bottom trawl was used on some adult SBW marks. This trawl used the same (50 m) sweeps and bridles but had a 60 mm mesh codend. The AOS was mounted on the hoki trawl due to its higher headline and provided a larger sampling volume for acoustical analysis of single targets.

Most target identification work was focused on:
1. establishing species mix proportions away from dominant heavy marks, which are easily identified as SBW;
2. confirming identification of other strong acoustic marks in the area as non-SBW (e.g., marks of silversides or oblique banded rattails);
3. distinguishing less dense adult marks from pre-recruit marks in areas where they occur in similar depths;
4. identifying the size and age composition of SBW in the less-dense, pre-recruit marks including 1, 2, and immature 3-year-old fish;
5. obtaining a sample of adult SBW in areas that were not being fished by the commercial fleet (e.g., this year the commercial fleet did not sample the southern aggregation).

Trawling was carried out both day and night. For each trawl, all items in the catch were sorted into species and weighed on Marel motion-compensating electronic scales accurate to about 0.1 kg. Where possible, finfish, squid, and crustaceans were identified to species level, and other benthic fauna to species or family level. A random sample of up to 200 SBW and 50–200 of other important species from every tow was measured. In most tows, the sex and macroscopic gonad stage (Appendix 4) of all SBW in the length sample were also determined. More detailed biological data were collected on a subsample of up to 20 SBW per trawl, and included fish length, weight, sex, gonad stage, gonad weight, and occasional observations on stomach fullness and contents, and prey condition. Otoliths were also collected from up to 20 SBW per trawl to augment those collected by the scientific observer programme, as well as to ensure that they were collected across the full survey area. Estimated SBW length frequencies from research trawls were constructed by scaling length frequencies from individual tows by the SBW catch in the tow.

2.4 Other data collection

A Seabird SM-37 Microcat CTD datalogger (serial number 2958) was mounted on the headline of the net during all 15 bottom trawls to allow calculation of the absorption coefficient and speed of sound for acoustic data processing (Appendix 5), and to define water mass characteristics in the area. CTD drops were also carried out in conjunction with the two acoustic calibrations.

2.5 Commercial catch data

Additional information on the species composition, size, and spawning state of adult SBW in the survey area was obtained from commercial catch data collected by scientific observers. Data from the 2019 fishery were extracted from the Fisheries New Zealand EDW database on 6 November 2019. Scaled length frequency distributions were calculated as the weighted (by catch) average of individual length samples. Data on female gonad stage (using the five-stage observer scale) were summarised by date.

2.6 Acoustic data analysis

Acoustic data collected during the survey were analysed using NIWA's open-source software ESP3 version 1.4.0 (Ladroit 2017). Data were visually inspected and carefully groomed, using a combination of automated algorithms and manual editing. The grooming included identifying artefacts (e.g., double bottom echoes, external interference), the "bottom line" (range in each ping beyond which data are affected by the bottom echo), and "bad transmits" (entire pings deemed to be unusable for analysis, due to interference, acoustic shadowing, or other process).

Marks were then identified, manually bounded by "region" polygons (interpretation masks) which were labelled by mark type. Consistent with previous surveys, SBW marks could be separated into adults (spawning fish) and immature (mainly 2-year olds). No juvenile (1-year old) marks were identified this year. The classification of marks was done subjectively by experienced scientists, using the mark appearance (shape, structure, strength, etc.), the context (time of day/night, depth, etc.), mark identification trawls, as well as descriptions available from previous years (Hanchet et al. 2003, O'Driscoll et al. 2018).

Acoustic backscatter data within regions labelled as SBW were then echo-integrated to produce acoustic density estimates (in m^2).In this process, we used a constant sound absorption of 9.41 dB km^{-1} and a constant sound velocity of 1484 m s^{-1}, based on CTD data collected during this survey (Appendix 5).

Total acoustic backscatter used for biomass estimation (section 2.7) was extracted by taking the average of the acoustic backscatter from each transect. Density maps were also obtained by slicing the transects in 10-ping bins, giving a resolution of about 100 m at survey speed of 10 knots (see section 3.4).

2.7 Biomass estimation

Acoustic density estimates for each transect were converted to SBW biomass using the ratio *r* of mean weight to mean backscattering cross-section (linear equivalent of target strength). Acoustic target strength was derived using the most recent target-strength-to-fork-length (TS - FL) relationship of O'Driscoll et al. (2013):

$$TS = 22.06 \log_{10} FL - 68.54 \qquad (2)$$

Where TS is in dB re 1 m^2 and FL in cm.

SBW biomass/weight w (in g) was determined using the combined length-weight relationship for spawning SBW from Hanchet (1991):

$$w = 0.00439\ FL^{3.133} \qquad (3)$$

Mean weight and mean backscattering cross-section (linear equivalent of TS) for each category (adult by area, and immature) were obtained by transforming the scaled length frequency distribution for both sexes combined by Equations 3 and 2 respectively, and then calculating the means of the transformed distributions.

Biomass estimates and variances were calculated from transect density estimates using the formulae of Jolly & Hampton (1990). The mean SBW stratum density for each category was multiplied by the stratum area to obtain biomass estimates for each stratum, which were then summed over all strata to produce an estimate for the snapshot. Finally, the values for the two snapshots were averaged to produce a biomass estimate for the survey. The sampling precision (CV) of the mean biomass estimate from the survey combined the variance from each snapshot, using the assumption that each snapshot was independent.

No towbody motion correction (Dunford 2005) was applied to biomass estimates, because measurements of towbody pitch and roll are not available for all surveys in the time-series. O'Driscoll et al. (2007) indicated that compensating for motion correction increased biomass by only 3–10% in 2006. As expected, the magnitude of the change due to motion correction was related to mark depth (larger effect with increasing depth) and sea conditions (larger effect in poor conditions when there was greater towbody motion).

2.8 Target strength measurements

Co-recording calibrated acoustic data and underwater video footage with identifiable fish and estimates of their length and tilt angle allows the *in situ* measurement of TS estimates. In this survey, acoustic data and co-registered videos were acquired using NIWA’s dual frequency Acoustic Optical System (AOS). The videos were taken using stereo machine vision cameras operating at a low frame rate (15 fps) to try to measure the tilt angle of individual fish using stereoscopic processing. These data were then matched with the acoustic data from the AOS sounders (Simrad 38 kHz narrow band and 90–170 kHz wideband). The AOS sounder was calibrated at depth on 20 September as it was being deployed on an SBW aggregation in “TS-probe” mode (Appendix 3).

In ESP3, “single targets” (echoes for individual fish) were detected, tracked over consecutive pings, and their backscatter value extracted for TS analysis. Table 3 lists the parameters used in the ESP3 “single target detection” and “single target tracking” algorithms. The mean TS of each track was then calculated to estimate the distribution of TS from the acoustic data and identify the possible modes corresponding to SBW.

3. RESULTS

3.1 Data collection

Survey objectives were achieved despite the loss of 145 hours (about 6 days) of survey time due to bad weather conditions. This was double the weather allowance of 3 days provided for in the survey design. Our arrival in the survey area was delayed because the vessel was slowed during transit to let a front pass, and thus the survey started on 3 September. The weather was relatively good during snapshot 1 and this snapshot was completed on 12 September, with the loss of only 19 hours. Shortly after starting snapshot 2, multiple fronts went through the area, leading to swells up to 12 m and winds up to 50 knots (Figure 5), and periods of work were alternated with periods of dodging the weather. On 16 September, a major front came through, and the vessel sheltered at Campbell Island for 60 hours. Work resumed on 18 September and snapshot 2 was finished on 21 September, with priority to the acoustic work, and little time for trawls and experimental work. The vessel left the survey area 24 hours early to avoid another major front that would have delayed its arrival in Wellington.

A total of 87 transects were run, including 55 with the towbody. The hull system was set to record continuously, with the 38 kHz echosounder in passive mode when the towbody was in the water to avoid acoustic interference. A total of 65 GB of acoustic data was recorded during the survey.

Fifteen research trawls were conducted for mark identification and collection of otoliths and biological data (Table 4). All trawls were carried out with bottom trawls, using either the ratcatcher (13 trawls) or the hoki trawl (2 trawls). Acoustic data were collected using the hull-mounted echosounders during trawls. Total catch was 2788 kg, composed of 87% SBW by weight. A total of 5500 fish of 34 different species, including 2853 SBW, were measured (Table 5). Otoliths were collected from 282 SBW for ageing.

Two deployments of the dual frequency, stereo-camera AOS were carried out (see Table 4). The first deployment was on 7 September, on the hoki trawl; and the second deployment was on 19 September as a lowered target strength probe, during which a deep calibration of its echosounders was conducted (Figure 6).

3.2 Commercial data

A total of 626 target SBW tows were reported by electronic catch reporting (ERS) from the Campbell Island grounds between 25 August and 1 October 2019, for a total estimated catch of 24 332 t of SBW. This was slightly lower than the reported (Monthly Harvest Return) catch of 26 308 t for SBW6I, and below the TACC of 39 200 t. Fishing effort was concentrated in the northern and eastern areas throughout the season, with 601 tows (23 561 t of SBW catch) in the north and 24 tows (770 t of SBW catch) in the east. At the time of this acoustic survey, fishing effort was mostly concentrated in strata 2 and 4, with some fishing from one vessel in 8E and 8S during the first snapshot (see Figure 4).

Two distinct spawning periods (defined as when the proportion of running ripe females exceeded 10%) were recorded, from 3–18 September and from 23–30 September (Figure 7). The timing of the first spawning in 2019 was similar to that in 2013 and 2016, and relatively early compared with the timing in other previous survey years.

The scaled length frequency distributions of SBW caught by commercial vessels are shown in Figure 8. Of the 626 commercial trawls, 242 trawls were carried out in the northern strata (strata 2, 3N, 3S, 4, 5) with 35 041 SBW measured; and 13 trawls were carried out in the eastern strata (strata 6N, 6S, 62, 8N, 8S, 8E, and 82) with 1840 SBW measured. Length distributions were bimodal for both males and females in the north, with the modes for males centred on 32 cm and 39 cm and the modes for females centred on about 33 cm and 42 cm. The length distributions in the east were generally similar, but the mean length of 37.3 cm for adult SBW in the east was slightly higher than that in the north at 36.8 cm (Table 6).

3.3 Mark identification

Mark types were similar to those described by Hanchet et al. (2002). Most adult marks can be identified by their overall shape and location in the water column.

In the first few days of snapshot 1, two separate aggregations were observed. The northern aggregation was first observed in stratum 4 on 4 September, around 51° 30’ S, 170° 10’ E in 450 m of water. An eastern aggregation was then detected on 7 September at the southern end of stratum 8S at 52° 34’ S, 171° 17’ E in 500 m of water. The northern aggregation seemed to be actively spawning, forming dense marks about 150 m above the bottom during the day (Figure 9). The eastern aggregation seemed to have spawned already and was more dispersed and possibly on the move (Figure 10).

A third aggregation was observed during snapshot 1, on the morning of 9 September, around 53° 30’ S, 169° 40' E at 500 m depth in stratum 7S. This southern aggregation was forming very dense schools on the bottom during daytime and large midwater marks during the night, which are typical of SBW during spawning (Figure 11). During snapshot 2, the southern aggregation was mainly composed of adults that remained in a similar area, strata 7S2 and 7N.

During both snapshots, immature SBW marks (Figure 12) were observed in depths shallower than 410 m. No juvenile marks were observed during this survey.

No species decomposition of acoustic backscatter was attempted because of the small number of trawls and uncertainty associated with the relative catchabilities of different species. All backscatter from adult and immature SBW marks was assumed to be from SBW consistent with previous years (Hanchet et al. 2003, Gauthier et al. 2011, O'Driscoll et al. 2007, 2012, 2014, 2018) and supported by the majority of previous trawl catches.

3.4 Spatial distribution of SBW backscatter

Spatial distribution of acoustic backscatter is shown in Figure 13 for adult SBW marks and in Figure 14 for immature SBW marks, for both snapshots. The northern adult aggregation was mainly within strata 2 and 4 and its location was similar between the two snapshots. The eastern aggregation appeared to have moved northwest in snapshot 2, joining partly with the northern aggregation. This was consistent with the spatial distribution of the commercial catch (see Figure 4). The two snapshots of the southern aggregation were closely spaced (in time) and this aggregation remained in the same area (Figure 13).

Immature SBW marks were only observed at depths shallower than 410 m. In snapshot 1, immature SBW were distributed along the southern border of stratum 2, the western border of strata 4, 5, and 7N (Figure 14). In snapshot 2, the distribution was similar but shifted southwards, with no marks in stratum 2 but some in the northern part of 7S2 (Figure 14).

3.5 SBW size and maturity

Length, sex, and stage were determined from 2853 SBW during the survey (Table 7). The scaled length frequencies from research trawls on adult and immature SBW marks are compared in Figure 8 and summarised in Table 6. The average size of adult SBW estimated from two research tows in the eastern aggregation (mean length 39.1 cm) was larger than that from tows in the northern aggregation (mean length 33.5 cm), but this might reflect the difference in selectivity between the different trawl gear types used in each area (tows in the east were carried out with the hoki trawl with 60 mm codend, and those in the north were with the ratcatcher with 40 mm codend). Because commercial length frequency data are thought to be more representative of the size of fish in the spawning aggregations, data from the commercial fishery were used to estimate *r* in the northern and eastern areas.

The length modes of fish from research tows on adult aggregations in the north and east were similar overall to those from the commercial catch (Figure 8). The southern aggregation seemed to have a higher proportion of small SBW than the other areas, but this observation is based only on research tows because there was no commercial catch on this aggregation. Fish caught from immature SBW marks had a single mode between 25 and 35 cm and were estimated to be 2 or 3 years old (2017 or 2016 year class).

The timing of spawning cannot be inferred from the research data because too few tows were carried out overall, and a significant proportion of them were outside the main spawning aggregations. Almost all adult female SBW caught in snapshot 1 were either pre-spawning (stage 3) or partially spent (stage 6), with the exception of the female SBW taken in stratum 7S on 9 September, which were mostly running ripe (stage 5). Males and females from marks classified as “immature” were almost exclusively at stage 1 (see Table 7).

3.6 SBW biomass estimates

Biomass estimates for SBW were calculated from acoustic density estimates using the weight-to-backscattering ratio *r* values in Table 6, which were computed using length frequency distributions shown in Figure 8. For immature SBW and for adult SBW from the southern area, the research trawl catch was used. For adult SBW of the northern and eastern areas, the commercial data were used.

Estimates of biomass by snapshot for adult and immature SBW are given by stratum in Table 8, and by general area in Table 9. The total adult biomass estimate was 119 175 t (CV 40%) in snapshot 1 and 63 115 t (CV 23%) in snapshot 2. The higher biomass and CV in snapshot 1 were due to a very dense spawning aggregation in one transect in stratum 7S (shown in Figure 11), which contributed 70% of the biomass in the southern area. However, unlike in 2016, the adult biomass estimates for each area (Figure 15), and overall (Figure 16), in 2019 were not significantly different between snapshots. At the Deepwater Working Group meeting of 30 October 2019, it was agreed to average the two snapshots to obtain the biomass index for 2019. The resulting average estimate of adult SBW biomass was 91 145 t (CV 27%).

The estimate of immature SBW biomass was 4100 t (CV 21%) in snapshot 1 and 4020 t (CV 31%) in snapshot 2, averaging to 4060 t (CV 18%). No juvenile biomass was estimated from this survey because no juvenile SBW marks were identified.

3.7 Target strength estimates

Both AOS deployments were carried out on relatively low-density aggregations, resulting in few targets being detected optically. Unfortunately, denser aggregations were encountered only during weather conditions that were unsuitable for AOS deployment. However, the stereo camera system has proven to work reliably and should be used in future surveys.

A total of 327 tracked targets were extracted from the AOS trawl deployment (station 8), and 1739 from the AOS TS-probe deployment (station 18, see Figure 6). On both deployments, no targets could be optically verified because the aggregation was not dense enough for the trawl and moved away from the probe (see Figure 6).

From the trawl data (station 8), few tracks in the range of TS expected for adult SBW (-30 to -40 dB) were detected (Figure 17). Fitting a 4-component Gaussian mixture to the distribution of mean TS recorded for the AOS TS-probe deployment (Figure 18) resulted in only 5% of the data attributable to a potential SBW mode (-35.2 dB mean).

No optically verified SBW were observed; therefore, no further work on target strength was carried out, because there was too much uncertainty in the identification of the acoustic targets.

4. DISCUSSION

4.1 Timing of survey

The timing and duration of the survey was similar to the previous seven surveys (Figure 7). Based on commercial catch data, there were two spawning events in 2019. The first event occurred during 3–18 September, which coincided with the start of snapshot 1 until midway into snapshot 2. The second spawning event was shorter and occurred during 23–30 September, which was slightly later than most years and after the end of the survey. The timing of the survey was therefore appropriate, encapsulating the entire first spawning event as well as the pre-spawning period of the second event.

4.2 Spatial coverage of survey

Historically, the Campbell SBW fishery has been characterised as occurring on two distinct aggregations, northeastern and southern, which often showed different fish length structure (Hanchet 1998, 2005). The location of the northeastern aggregation has varied over the years. Since 2002, there has been increasing commercial fishing effort outside the historical core survey area (strata 2 to 7, e.g., Figure 1). Hanchet (2005) examined commercial length frequency data from 1997 to 2004, found that SBW caught east of the core area had a similar size distribution to those caught in the north within the core area, and concluded that changes in fish spatial distribution were likely due to fish movement rather than the existence of a unrecorded population. In 2011 and 2013, rather than the single northeast aggregation observed previously, two distinct aggregations were observed in the north and in the east (O'Driscoll et al. 2012, 2014), and the spatial distribution of commercial catch in 2011, 2012 and 2015 provides additional evidence of this geographical split (see Figure 1).

At the same time as the distribution of SBW appeared to have spread out in the northeast, the relative contribution of the southern aggregation declined. In 2009, very dense spawning marks were detected in the south, resulting in the southern aggregation accounting for 24% of the estimated adult acoustic biomass on the Campbell Island Rise (Gauthier et al. 2011). In 2011, this proportion declined to only 3% of the estimated adult biomass (O'Driscoll et al. 2012). In 2013, despite extensive searching, no spawning SBW were detected in the south (O'Driscoll et al. 2014). Commercial data confirmed this decline, with catch rates in the south progressively declining to only 5 trawls in this area in 2013. The aggregation then seems to have reappeared with catch taken from the south in 2014–16 (see Figure 1).

In 2016, the acoustic survey observed three separate adult aggregations, in the north, east, and south. Most commercial fishing effort was in the east and south, but dense acoustic marks were observed in the northern area in both snapshots (O'Driscoll et al. 2018).

In 2019, the three adult aggregations were detected again. The estimated relative contribution of the three areas to the 'best' adult acoustic abundance estimates in 2019 was: north, 23%; east, 25%; and south, 52% (see Table 9). The southern aggregation contributed a much higher proportion of the total biomass than in 2016 when it was only 8% of the adult abundance. This large proportion of the southern aggregation in 2019 was influenced by one particularly dense mark during snapshot 1, but this observation was later confirmed with the southern aggregation still contributing 43% of the adult biomass in snapshot 2.

There were no clear differences in fish size between the northern and eastern aggregations based on commercial length frequency data (Figure 8). Comparison of size composition between areas from research data was difficult because of the small number of tows and the use of different trawl gears. However, a higher proportion of smaller fish were observed in the south (see Figure 8).

In light of the continuing changes in the spatial distribution of SBW, the survey area and stratification should continue to be reviewed before future surveys.

4.3 Variability between snapshot

The estimated adult biomass in snapshot 1 was nearly double that in snapshot 2. Most of this difference was due to one dense mark on transect 3 of stratum 7S (Figure 11). This mark was sampled (station 14) and the tow caught 95% of spawning SBW (Table 3). This single mark contributed over 70% of the estimated adult biomass in stratum 7S, resulting in a high CV (78%) for this snapshot. Despite this, the adult biomass estimates, whether for each area or overall (Figure 15), were not significantly different between snapshots. The Deepwater Working Group agreed to average the two snapshots to obtain the biomass indices for 2019.

In 2016, there was a four-fold difference in adult SBW biomass estimates between snapshots 1 and 2, which is greater than in any of the other surveys in the Campbell time series. The maximum difference that had been observed previously was a factor of 2.5 in 2002 (Figure 16). The 2016 survey was also the only one where the two snapshot estimates did not have overlapping 95% confidence intervals. This was because only weak adult marks were detected in the east in snapshot 1, whereas extensive post-spawning marks were detected a week later in snapshot 2 (O'Driscoll et al. 2018). O'Driscoll et al. (2018) explored various hypotheses to explain the low estimated biomass of adult SBW in the eastern area during snapshot 1 in 2016 and noted that it was not statistically appropriate to average abundance estimates from this region from the two snapshots. The Deepwater Fisheries Assessment Working Group agreed that the 'best' estimate of adult SBW biomass in 2016 was calculated by averaging the two snapshot estimates for the northern and southern aggregations and adding the snapshot 2 estimate for the eastern aggregation.

The estimates of immature SBW were very consistent between snapshots in 2019 (Table 8), although the spatial distribution differed slightly (Figure 14).

4.4 Comparison between years

Total estimated biomass for adult SBW in 2019 decreased slightly (by 6%) from 2016 but was the fourth highest in the time series. This is consistent with relatively good recent recruitment and recent catches well below the TACC. The 2006, 2009, and 2011 year classes have been estimated as being relatively strong (Large et al. in press) and SBW from these year classes probably account for many of the larger fish caught in 2019. The smaller SBW caught in 2019 were fish from the 2014 and 2015 year classes (ages 5 and 4 respectively, NIWA unpublished data).

The estimated abundance of immature SBW in 2019 was similar to that in 2016 and below average for the time series. This suggests that the 2016 and 2017 year classes (ages 3 and 2, respectively) were not abundant. Although they were not well indexed by the survey because they also occur in shallower depths outside of the survey area, no juvenile SBW were observed in 2019; this suggests that the 2018 year class (age 1) was not abundant.

5. ACKNOWLEDGMENTS

Thanks to the officers, crew, and scientific staff of *Tangaroa* for making this a successful voyage in this sometimes-harsh sub-Antarctic environment. Diving Services New Zealand Ltd provided dive support for the acoustic calibration in the Marlborough Sounds. We are also grateful to skippers, fishing masters, and company representatives on other vessels fishing on the Campbell grounds for providing and sharing information. This research was funded by Fisheries New Zealand project SBW2019/01. Alexandre Schimel (NIWA) reviewed a draft of this report and made several helpful comments.

6. REFERENCES

Demer, D.A.; Berger, L.; Bernasconi, M.; Bethke, E.; Boswell, K.; Chu, D.; Domokos, R., et al. (2015). Calibration of acoustic instruments. *ICES Cooperative Research Report No. 326*. 133 p.

Doonan, I.J.; Coombs, R.F.; McClatchie, S. (2003). The absorption of sound in seawater in relation to the estimation of deep-water fish biomass. *ICES Journal of Marine Science 60*: 1047–1055.

Dunford, A. (2005). Correcting echo integration data for transducer motion. *Journal of the Acoustical Society of America 118*: 2121–2123.

Dunford, A.J.; Macaulay, G.J. (2006). Progress in determining southern blue whiting (*Micromesistius australis*) target strength: results of swimbladder modelling. *ICES Journal of Marine Science 63*: 952–955.

Dunn, A.; Grimes, P.J.; Hanchet, S.M. (2001). Comparative evaluation of two-phase and adaptive cluster sampling designs for acoustic surveys of southern blue whiting (*M. australis*) on the Campbell Rise. Final Research Report for Ministry of Fisheries Research Project SBW1999/01. Objective 1. 15 p. (Unpublished report held by Fisheries New Zealand, Wellington.)

Dunn, A.; Hanchet, S.M. (1998). Two-phase acoustic survey designs for southern blue whiting on the Bounty Platform and the Pukaki Rise. *NIWA Technical Report 28*. 29 p.

Fofonoff, P.; Millard, R.Jr. (1983). Algorithms for computation of fundamental properties of seawater. *UNESCO Technical Papers in Marine Science 44*. 53 p.

Francois, R.E.; Garrison, G.R. (1982). Sound absorption based on ocean measurements. Part II: Boric acid contribution and equation for total absorption. *Journal of the Acoustical Society of America 72*: 1879–1890.

Fu, D.; Hanchet, S.; O'Driscoll, R.L. (2013). Estimates of biomass and c.v.s of southern blue whiting from previous acoustic surveys from 1993 to 2012 using a new target strength – fish length relationship. Final Research Report for Ministry for Primary Industries Research Project DEE201002SBWB. 52 p. (Unpublished report held by Fisheries New Zealand, Wellington.)

Gauthier, S.; Fu, D.; O'Driscoll, R.L.; Dunford, A. (2011). Acoustic estimates of southern blue whiting from the Campbell Island Rise, August–September 2009. *New Zealand Fisheries Assessment Report 2011/9*. 40 p.

Hanchet, S.M. (1991). Southern blue whiting fishery assessment for the 1991–92 fishing year. New Zealand Fisheries Assessment Research Document 91/7. 48 p. (Unpublished report held by NIWA library, Wellington.)

Hanchet, S.M. (1998). A review of southern blue whiting (*Micromesistius australis*) stock structure. New Zealand Fisheries Assessment Research Document 98/8. 28 p. (Unpublished report held by NIWA library, Wellington.)

Hanchet, S.M. (1999). Stock structure of southern blue whiting (*Micromesistius australis*) in New Zealand waters. *New Zealand Journal of Marine and Freshwater Research 33*: 599–610.

Hanchet, S.M. (2005). Southern blue whiting (*Micromesistius australis*) stock assessment update for the Campbell Island Rise for 2005. *New Zealand Fisheries Assessment Report 2005/40*. 40 p.

Hanchet, S.M.; Bull, B.; Bryan, C. (2000). Diel variation in fish density estimates during acoustic surveys of southern blue whiting. *New Zealand Fisheries Assessment Report 2000/16*. 22 p.

Hanchet, S.M.; Grimes, P.J.; Coombs, R.F.; Dunford, A. (2003). Acoustic biomass estimates of southern blue whiting (*Micromesistius australis*) for the Campbell Island Rise, August-September 2002. *New Zealand Fisheries Assessment Report 2003/44*. 38 p.

Hanchet, S.M.; Grimes, P.J.; Dunford, A.; Ricnik, A. (2002). Classification of fish marks from southern blue whiting acoustic surveys. Final Research Report for Ministry of Fisheries Research Project SBW2000/02 Objective 2. 55 p. (Unpublished report held by Fisheries New Zealand, Wellington.)

Jolly, G.M.; Hampton, I. (1990). A stratified random transect design for acoustic surveys of fish stocks. *Canadian Journal of Fisheries and Aquatic Sciences 47*: 1282–1291.

Ladroit, Y. (2017). ESP3. Available online at: https://sourceforge.net/projects/esp3/

Large, K.; O'Driscoll, R.L.; Schimel, A.C.G. (in press). Review and summary of the time series of input data available for the assessment of southern blue whiting (*Micromesistius australis*) stocks up to and including the 2018 season. New Zealand Fisheries Assessment Report.

MacLennan, D.N. (1981). The theory of solid spheres as sonar calibration targets. *Scottish Fisheries Research 22*. 17 p.

O'Driscoll, R.L. (2011). Acoustic biomass estimates of southern blue whiting on the Pukaki Rise and Campbell Island Rise in 2010. NIWA Client Report WLG2011-03 for The Deepwater Group Ltd. 37 p. (Unpublished report available from Deepwater Group Ltd, Auckland)

O'Driscoll, R.L.; Dunford, A.J.; Fu, D. (2012). Acoustic estimates of southern blue whiting from the Campbell Island Rise, August–September 2011 (TAN1112). *New Zealand Fisheries Assessment Report 2012/18*. 52 p.

O'Driscoll, R.L.; Dunford, A.J.; Ladroit, Y. (2014). Acoustic estimates of southern blue whiting from the Campbell Island Rise, August–September 2013 (TAN1309). *New Zealand Fisheries Assessment Report 2014/22*. 46 p.

O’Driscoll, R.L.; Hanchet, S.M. (2004). Acoustic survey of spawning southern blue whiting on the Campbell Island Rise from FV *Aoraki* in September 2003. *New Zealand Fisheries Assessment Report 2004/27*. 31 p.

O'Driscoll, R.L.; Hanchet, S.M.; Gauthier, S.; Grimes, P.J. (2007). Acoustic estimates of southern blue whiting from the Campbell Island Rise, August-September 2006. *New Zealand Fisheries Assessment Report 2007/20.* 34 p.

O’Driscoll, R.L.; Large, K.; Marriott, P. (2018). Acoustic estimates of southern blue whiting from the Campbell Island Rise, August–September 2016 (TAN1610). *New Zealand Fisheries Assessment Report 2018/56*. 60 p.

O'Driscoll; R.L.; Macaulay, G.J.; Gauthier, S. (2006). Biomass estimation of spawning southern blue whiting from industry vessels in 2006. NIWA Client Report: WLG2006-89 for the Deepwater Stakeholders Group Ltd. 43 p. (Unpublished report available from Deepwater Group Ltd, Auckland).

O’Driscoll, R. L.; Oeffner, J.; Dunford, A.J. (2013). *In situ* target strength estimates of optically verified southern blue whiting (*Micromesistius australis*). *ICES Journal of Marine Science 70*: 431–439.

Pedersen, G.; Godø, O.R.; Ona, E.; Macaulay, G.J. (2011). A revised target strength–length estimate for blue whiting (*Micromesistius poutassou*): implications for biomass estimates. *ICES Journal of Marine Science 68*: 2222–2228.

7. TABLES

Table 1: Summary of transects and trawls carried out during snapshot 1 of the 2019 SBW acoustic survey of the Campbell Island Rise. Transect positions are plotted in Figure 2. Strata 2–7 are core strata which have been surveyed in all previous acoustic surveys.

		Number of transects		
Stratum	Area (km2)	Planned	Completed	Number of trawls
2	3 154	5	5	2
3N	2 342	3	3	0
3S	1 013	3	3	0
4	2 690	5	5	3
5	3 029	4	4	1
6N	1 150	4	3	0
6S	3 025	3	3	0
7N	2 980	4	4	3
7S	3 815	8	8	1
8N	1 436	3	3	0
8S	1 979	3	4	3
8E	4 648	6	6	0
Total	31 261	51	51	13

Table 2: Summary of transects and trawls carried out during snapshot 2 of the 2019 SBW acoustic survey of the Campbell Island Rise. Transect positions are plotted in Figure 3.

Stratum	Area (km2)	Number of transects	Number of trawls
2	3 154	3	0
3S	1 013	3	0
4	2 690	5	0
5	3 029	3	1
62	2 500	6	0
7N	2 980	4	0
7S2	2 107	6	2
82	5 066	6	0
Total	22 539	36	3

Table 3: Parameters used in ESP3 for single target detection and tracking of targets.

Single Target Detection for split-beam echosounder parameters		
TS threshold (min)	-70	dB
TS threshold (max)	-15	dB
Pulse length determination level	12	dB
Minimum normalized pulse length	0.7	
Maximum normalized pulse length	1.2	
Maximum Beam compensation	9	dB
Max STD for Minor Axis Angle	1	degree
Max STD for Major Axis Angle	1	degree
Fish Track detection parameters		
Alpha (range, major and minor axis)	0.7	
Beta (range, major and minor axis)	0.5	
Exclusion distance (major and minor axis)	1	m
Exclusion distance (range)	0.5	m
Missed ping expansion (range, major and minor axis)	5	%
Major and minor axis weight	20	%
Range weight	50	%
TS weight	10	%
Angular uncertainties (major and minor axis)	1	degree
Minimum number of single targets in track	10	
Minimum number of pings in track	12	pings
Maximum gap between single targets	2	pings

Table 4: Station details and catch of SBW during the 2019 acoustic survey of the Campbell Island Rise. Station positions are plotted in Figure 2 and Figure 3. In the gear column: "RC" stands for ratcatcher trawl; "HT" for hoki trawl; "HT/AOS" for open cod-end hoki trawl with AOS attached; and "AOS", for AOS in TS-Probe mode. In the mark type column: "Adult" stands for adult SBW; "Immature" for immature SBW; and "CAS" for oblique banded rattail. --- indicates no catch taken.

Station	Date	Gear	Mark type	Stratum	Latitude (°)	Longitude (°)	Depth (m)	Distance (nm)	SBW biomass (kg)	Total biomass (kg)	SBW biomass proportion (%)
2	3-Sep-19	RC	Immature	2	-51.70	169.68	319	0.56	63.8	85.0	75
3	4-Sep-19	RC	CAS	2	-51.76	169.90	317	0.58	0.0	24.8	0
4	5-Sep-19	RC	Immature	4	-51.79	170.09	351	0.55	3.5	14.9	23
5	5-Sep-19	RC	Adult	4	-51.72	170.36	440	0.43	119.0	140.7	85
6	5-Sep-19	RC	Adult	4	-51.80	170.63	465	0.65	91.4	160.8	57
7	6-Sep-19	HT	Adult	8S	-52.40	171.38	551	0.92	54.6	64.8	84
8	7-Sep-19	HT/AOS	Adult	8S	-52.41	171.22	110	0.15	----	-----	----
9	7-Sep-19	HT	Adult	8S	-52.57	171.37	511	0.3	222.9	236.8	94
10	8-Sep-19	RC	Immature	5	-52.24	170.29	355	0.62	43.3	51.0	85
11	9-Sep-19	RC	Immature	7N	-52.83	170.19	411	0.21	543.3	552.9	98
12	9-Sep-19	RC	Immature	7N	-52.82	170.12	235	0.73	11.2	42.8	26
13	9-Sep-19	RC	Adult	7N	-52.82	170.25	431	0.47	67.6	75.9	89
14	10-Sep-19	RC	Adult	7S	-53.40	169.93	530	0.07	468.4	492.7	95
15	12-Sep-19	RC	Adult	7S2	-53.31	170.07	475	0.13	108.8	124.9	87
16	14-Sep-19	RC	Adult	7S2	-53.22	170.24	454	0.57	335.6	392.1	86
17	15-Sep-19	RC	Immature	5	-52.51	170.23	423	0.41	279.0	327.8	85
18	19-Sep-19	AOS	Adult	62	-51.79	170.72	400	2.23	----	----	----

Table 5: Trawl catch and number of fish measured during the 2019 acoustic survey of the Campbell Island Rise. [Continued on the next page]

Code	Scientific Name	Common name	Catch weight (kg)	Number measured
ACS	Actinostolidae	Smooth deepsea anemones	0.3	0
API	*Alertichthys blacki*	Alert pigfish	0.8	13
BOC	*Bolocera* spp.	Deepsea anemone	0.2	0
CAM	*Camplyonotus rathbunae*	Sabre prawn	0.6	0
CAS	*Coelorinchus aspercephalus*	Oblique banded rattail	114.5	1 105
CFA	*Coelorinchus fasciatus*	Banded rattail	0.2	5
COL	*Coelorinchus oliverianus*	Olivers rattail	0.2	1
DCO	*Notophycis marginata*	Dwarf cod	0.9	62
DCS	*Bythaelurus dawsoni*	Dawson's catshark	0.1	0
DHU	*Diaphus hudsoni*	Hudson's lanternfish	0.1	3
DSP	*Congiopodus coriaceus*	Deepsea pigfish	7.3	74
EZE	*Enteroctopus zealandicus*	Yellow octopus	0.8	0
GLO	*Glyphocrangon lowryi*	Goblin prawn	0.1	0
GSC	*Jacquinotia edwardsii*	Giant spider crab	11.1	0
GSH	*Hydrolagus novaezealandiae*	Ghost shark	1.5	1
GSP	*Hydrolagus bemisi*	Pale ghost shark	2.2	1
GYM	*Gymnoscopelus* spp.	*Gymnoscopelus* spp	0.1	3
HAK	*Merluccius australis*	Hake	32.6	4
HCO	*Bassanago hirsutus*	Hairy conger	0.5	4
HMT	Hormathiidae	Deepsea anemone	1.4	0
HOK	*Macruronus novaezelandiae*	Hoki	6.6	2
HYA	*Hyalascus* sp.	Floppy tubular sponge	60.2	0
JAV	*Lepidorhynchus denticulatus*	Javelin fish	27.7	720
LAN	Myctophidae	Lantern fish	0.3	0
LHE	*Lampanyctodes hectoris*	Hector's lanternfish	0.2	0
LIN	*Genypterus blacodes*	Ling	13.8	9
MAN	*Neoachiropsetta milfordi*	Finless flounder	1.6	2
MIQ	*Onykia ingens*	Warty squid	2.6	0
MMU	*Maurolicus australis*	Pearlside	0.1	0
MNI	*Munida* spp.	Munida unidentified	0.1	0
MOD	Moridae	Morid cods	1.3	30
NCB	*Nectocarcinus bennetti*	Smooth red swimming crab	8.0	0
NOS	*Nototodarus sloanii*	NZ southern arrow squid	9.0	94
ONG	Porifera	Sponges	1.1	0
OPA	*Hemerocoetes* spp.	Opalfish	1.3	31
OPI	*Opisthoteuthis* spp.	Umbrella octopus	0.2	0
PAG	Paguroidea	Pagurid	0.1	0
PHO	*Phosichthys argenteus*	Lighthouse fish	0.1	1
PLY	*Polycheles* spp.	Polychelidae	0.2	0
PRA		Prawn	0.3	0
PRO	*Protomyctophum* spp.	*Protomyctophum* spp	0.2	10

PYR	*Pyrosoma atlanticum*	*Pyrosoma atlanticum*	2.2	0
RCO	*Pseudophycis bachus*	Red cod	2.9	3
RSK	*Zearaja nasuta*	Rough skate	2.5	2
SAL		Salps	0.5	0
SBW	*Micromesistius australis*	Southern blue whiting	2 412.4	2 853
SCD	*Notothenia microlepidota*	Smallscaled cod	6.9	5
SCO	*Bassanago bulbiceps*	Swollenhead conger	0.4	2
SDF	*Azygopus pinnifasciatus*	Spotted flounder	0.6	19
SMK	*Teratomaia richardsoni*	Spiny masking crab	0.2	0
SPD	*Squalus acanthias*	Spiny dogfish	2.4	2
SQX		Squid	0.1	0
SSI	*Argentina elongata*	Silverside	43.2	437
SSK	*Dipturus innominatus*	Smooth skate	2.0	1
TOP	*Ambophthalmos angustus*	Pale toadfish	1.0	1
VNI	*Lucigadus nigromaculatus*	Blackspot rattail	0.1	0
		Total	2 787.9	5 500

Table 6: Estimates of the ratio r used to convert SBW backscatter to biomass. Values are derived from the scaled length frequency distributions in Figure 8. Abundance estimates (Table 8) were calculated using r from commercial tows for adult SBW in the northern and eastern areas, and from research tows for immature SBW and for adult SBW in the southern area where there was almost no commercial fishing (only 1 tow). σ is the acoustic backscattering coefficient.

Category	Data source	No. of trawls measured	Mean length (cm)	Mean weight (g)	Mean σ (m^2)	Mean TS (dB)	r (kg m^{-2})
Adult (north)	Commercial	601	36.8	383	0.000411	-33.9	929
Adult (east)	Commercial	24	37.3	397	0.000423	-33.7	940
Adult (north)	Research	2	33.5	276	0.000330	-34.8	836
Adult (east)	Research	2	39.1	448	0.000463	-33.3	966
Adult (south)	Research	4	32.7	260	0.000315	-35.0	827
Immature	Research	6	29.2	173	0.000240	-36.2	721

Table 7: Gonad stages of SBW caught in research trawls during the 2019 acoustic survey. Gonad stages are defined in Appendix 4. Mark types are as defined in Table 4.

					Males							Females						
Tow	Date	Stratum	Mark type	Stage	1	2	3	4	5	6	7	1	2	3	4	5	6	7
2	3-Sep-19	2	Immature		37	56	13	0	1	0	0	170	11	6	1	0	0	0
3	3-Sep-19	2	CAS		0	0	0	0	0	0	0	0	0	2	0	0	0	0
4	4-Sep-19	4	Immature		19	0	0	0	0	0	0	4	0	0	0	0	0	0
5	5-Sep-19	4	Adult		3	49	54	10	0	0	0	4	28	84	3	0	6	0
6	5-Sep-19	4	Adult		0	1	47	50	12	26	0	1	0	41	5	1	27	6
7	5-Sep-19	8S	Adult		0	0	17	33	21	48	1	1	1	11	0	1	34	3
9	6-Sep-19	8S	Adult		0	0	1	27	39	58	0	0	0	67	2	0	30	3
10	7-Sep-19	5	Immature		40	8	5	0	0	0	0	172	2	0	0	0	0	0
11	8-Sep-19	7N	Immature		25	4	11	19	13	25	0	73	1	10	2	0	23	0
12	9-Sep-19	7N	Immature		10	2	12	2	0	3	0	27	3	4	0	0	4	0
13	9-Sep-19	7N	Adult		0	2	13	19	30	50	1	1	5	10	0	2	46	3
14	9-Sep-19	7S	Adult		0	0	0	4	51	34	2	0	0	8	34	111	7	3
15	10-Sep-19	7S2	Adult		0	0	0	0	0	13	24	1	0	2	1	2	51	163
16	12-Sep-19	7S2	Adult		1	9	38	25	26	48	49	0	14	15	1	0	18	18
17	14-Sep-19	5	Immature		68	8	7	0	0	1	2	198	1	2	0	0	0	2

Table 8: Abundance estimates (t) and CV (%) by stratum and snapshot for immature and adult SBW for the Campbell Island Rise in 2019.

	Immature		Adult	
Stratum	Biomass (t)	CV (%)	Biomass (t)	CV (%)
Snapshot 1				
2	634	81	736	43
3N	0	–	0	–
3S	0	–	0	–
4	225	64	19 270	11
5	1 672	23	0	–
6N	0	–	323	100
6S	0	–	0	–
7N	1 569	34	9 382	19
7S	0	–	58 295	78
8E	0	–	4 045	33
8N	0	–	858	100
8S	0	–	26 266	54
Total	4 100	21	119 175	40
Snapshot 2				
2	0	–	2 343	23
3S	0	–	805	54
4	477	36	13 097	31
5	2 309	43	5 965	77
62	0	–	7 052	27
7N	441	100	8 307	27
7S2	793	68	18 613	48
82	0	–	6 934	46
Total	4 020	31	63 115	23
Average	4 060	18	91 145	27

Table 9: Final biomass summary by sub-areas for adult SBW on the Campbell Island Rise in 2019. The biomass is in tonnes with CV (%) in parentheses.

	Snapshot 1	Snapshot 2	Average
All	119 175 (40)	63 115 (19)	91 145 (27)
Core	88 005 (52)	56 181 (20)	72 093 (33)
North	20 005 (10)	22 209 (28)	21 107 (15)
East	31 493 (45)	13 986 (27)	22 739 (32)
South	67 677 (67)	26 919 (34)	47 298 (49)

Table 10: Biomass estimates (t) by survey and mark type for the Campbell Island Rise. Values for surveys from 1993–2011 are from Fu et al. (2013) and all were calculated using estimates of TS from O'Driscoll et al. (2013).

	Juvenile	CV (%)	Immature	CV (%)	Adult	CV (%)
1993	0	–	35 208	25	16 060	24
1994	0	–	8 018	38	72 168	34
1995	0	–	15 507	29	53 608	30
1998	322	45	6 759	20	91 639	14
2000	423	39	1 864	24	71 749	17
2002	1 969	39	247	76	66 034	68
2004	639	67	5 617	16	42 236	35
2006	504	38	3 423	24	43 843	32
2009	0	–	24 479	26	99 521	27
2011	0	–	14 454	17	53 299	22
2013	0	–	8 004	55	65 801	25
2016	775	37	4 456	19	97 117	16
2019	0	–	4 060	18	91 145	27

8. FIGURES

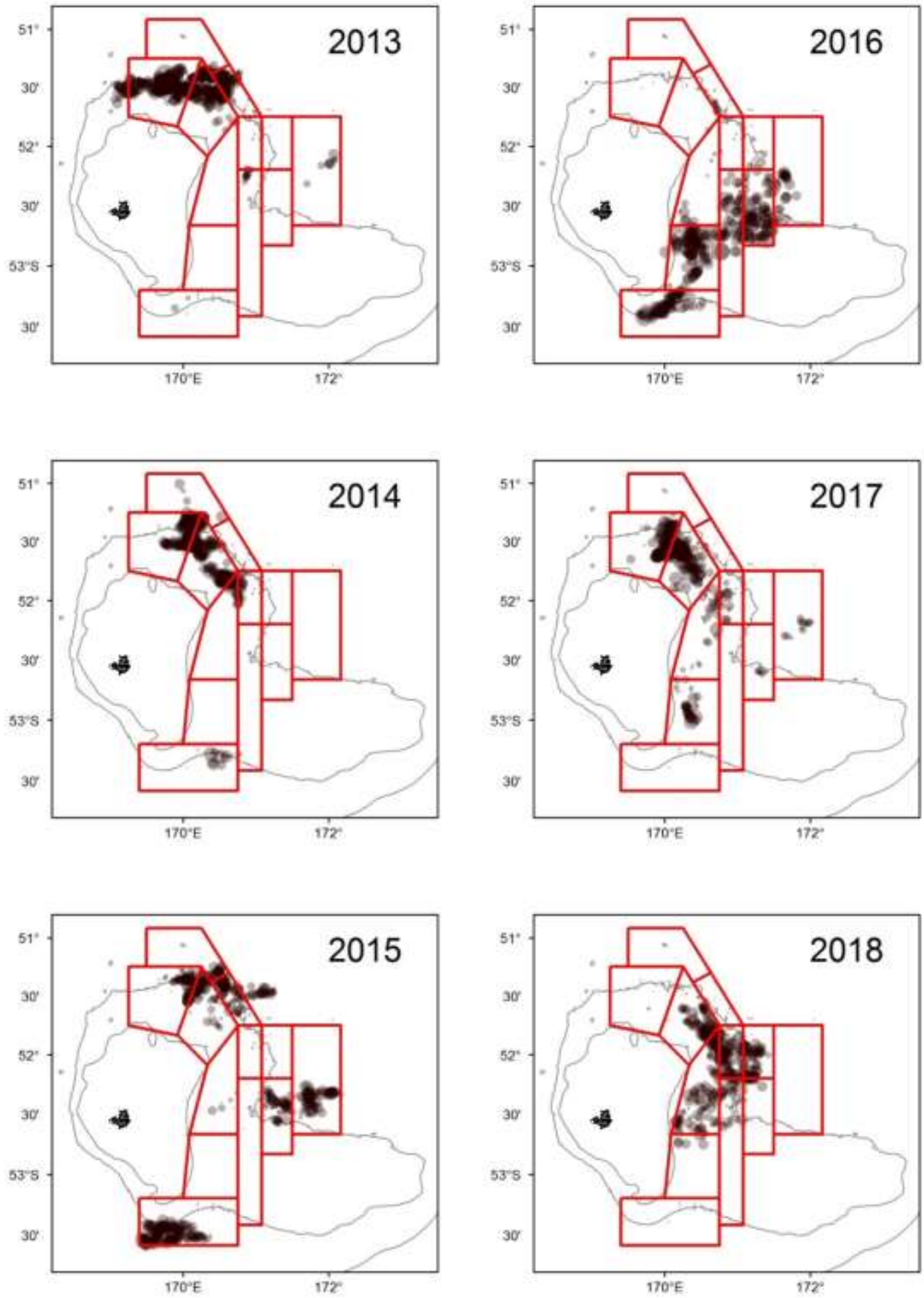

Figure 1: Stratum boundaries for Snapshot 1 of the 2019 acoustic survey superimposed on plots of catch rates from commercial trawls on the Campbell Island Rise from 2013–18. Circle area is proportional to SBW catch rate.

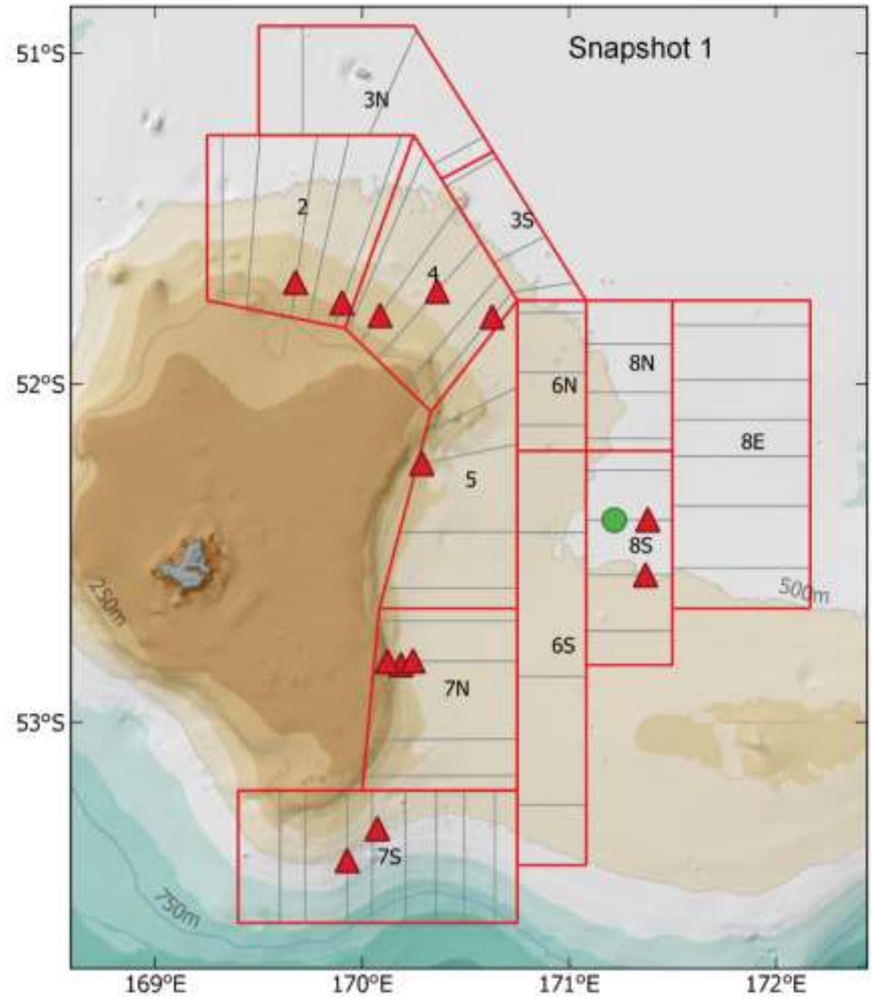

Figure 2: Location of stratum boundaries (red lines), acoustic transects (grey lines), and sampling stations during snapshot 1 on 3-12 September 2019. Red triangles are bottom trawls, and the green circle is the AOS deployment on trawl.

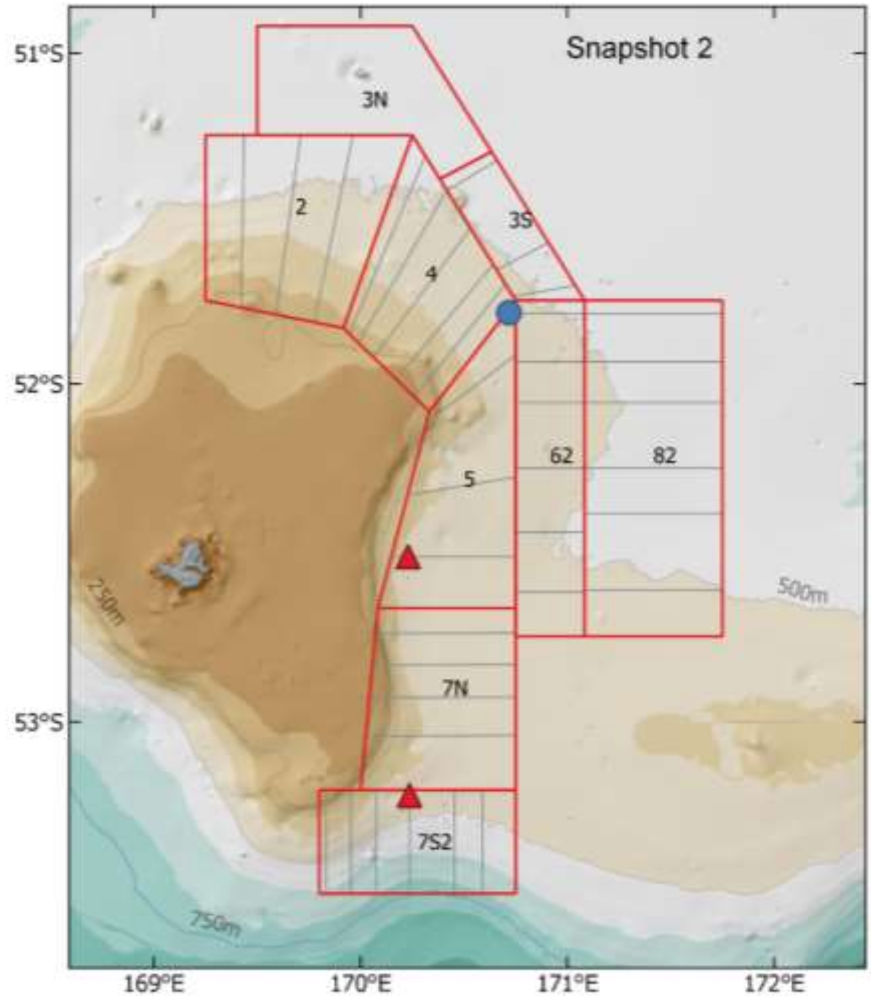

Figure 3: Location of stratum boundaries (red lines), acoustic transects (grey lines), and sampling stations during snapshot 2 on 12-21 September 2019. Red triangles are bottom trawls, and the blue circle is the AOS deployment.

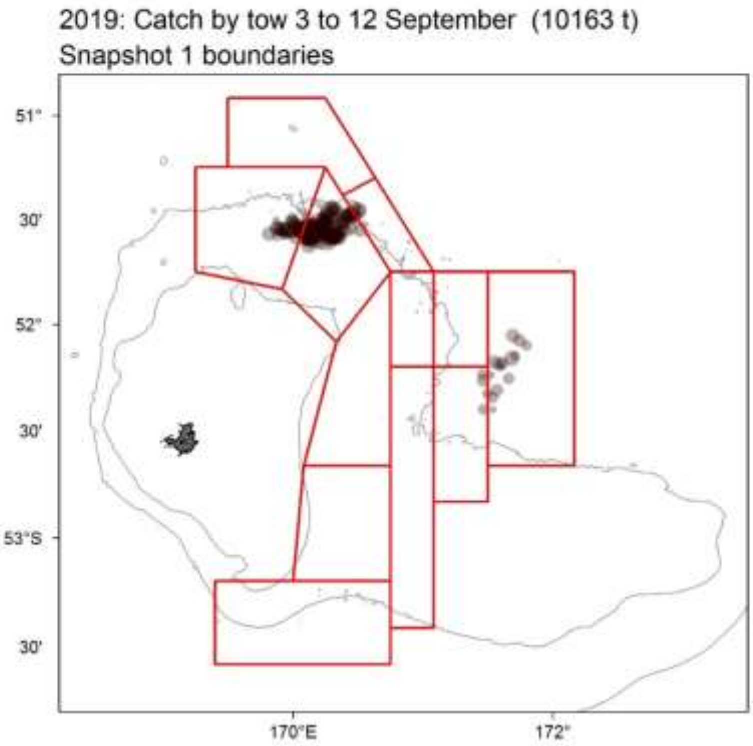

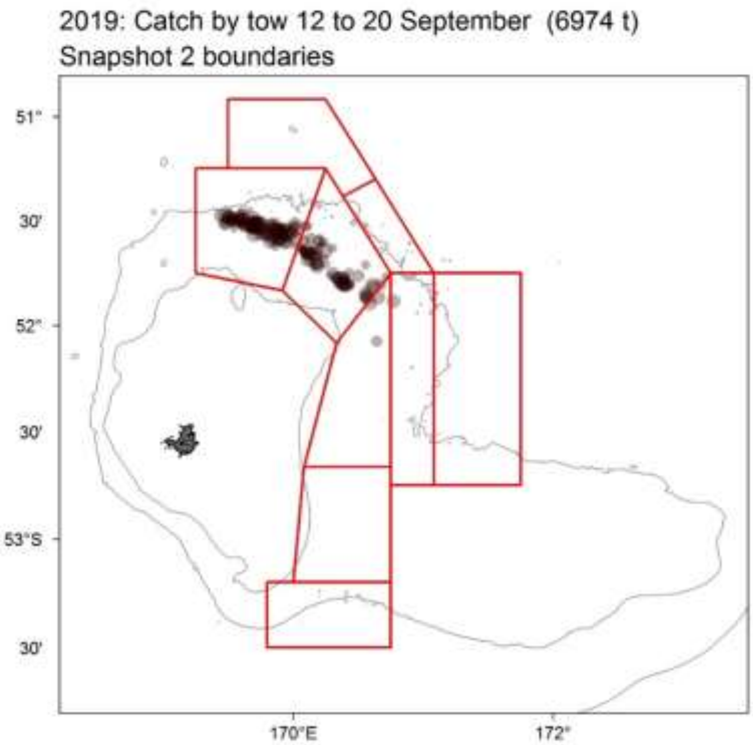

Figure 4: Stratum boundaries for snapshot 1 (upper panel) and snapshot 2 (lower panel) of the 2019 acoustic survey of the Campbell Island Rise superimposed on plots of catch rates from commercial trawls carried out during each snapshot. Circle area is proportional to SBW catch rate. Refer to Figures 2 and 3 for areas.

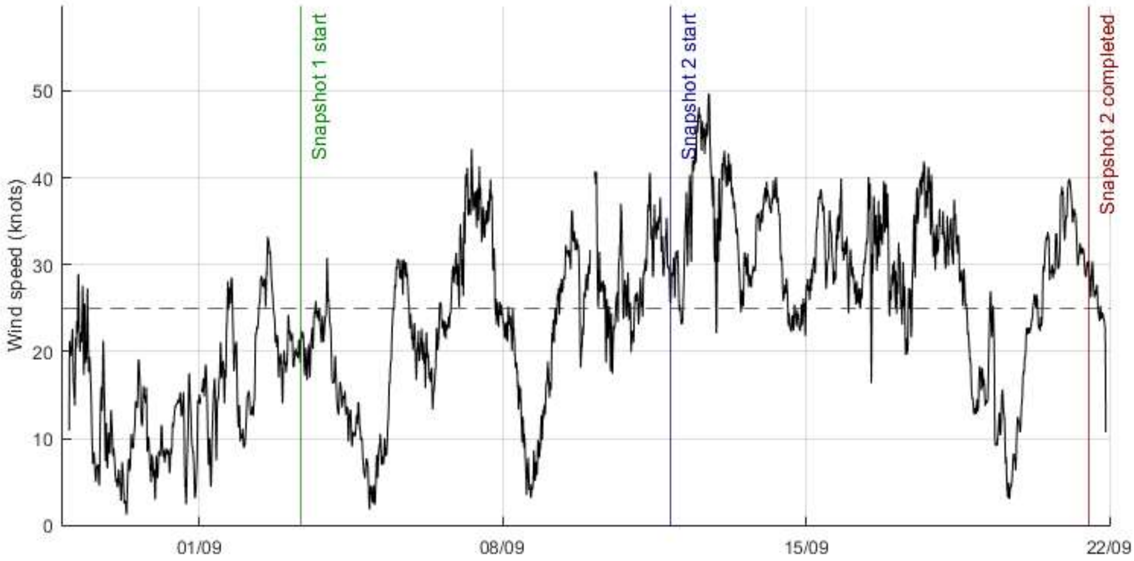

Figure 5: Output from *Tangaroa* data acquisition system (DAS) showing mean hourly wind speed during the survey. Data are true wind speed (i.e., corrected for relative motion of ship). The dashed line indicates 25 knots, which is considered as a maximum threshold for collection of acoustic data with hull-mounted transducer.

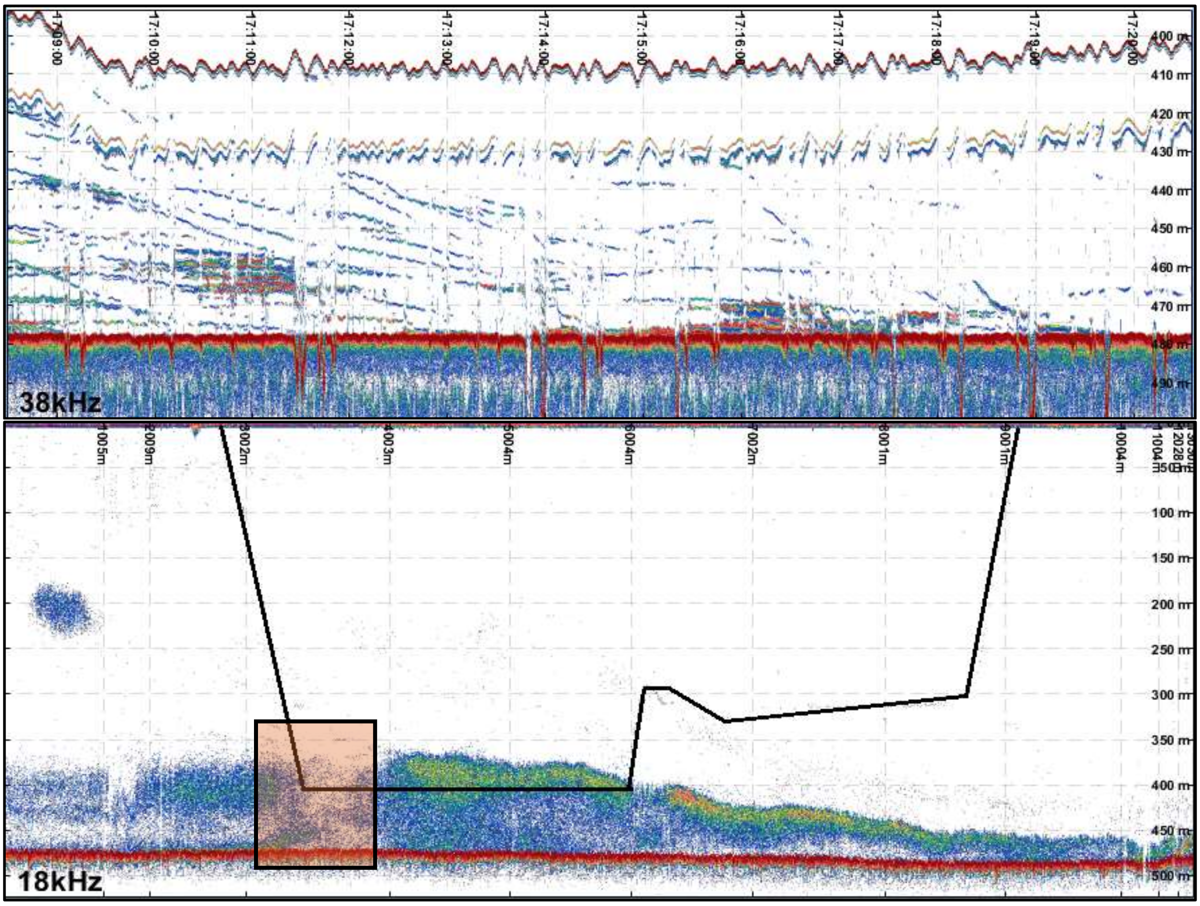

Figure 6: The Acoustic Optical System (AOS) being lowered on a SBW mark as a TS probe. The AOS was kept in the mark, recording stereo camera photos and dual-frequency acoustic data (38 kHz narrowband and 90-170 kHz wideband). Top: AOS 38 kHz sounder data from the start of the deployment, showing calibration sphere echoes about 20 m below transducer (wiggly line at 400-410 m). Calibration weight is at 420-430 m. Seabed is at about 480 m. Individual fish targets are observed diving away from the AOS (slanted horizontal lines). Bottom: Hull 18 kHz sounder data showing the AOS depth path (black line) within the SBW mark. The orange square shows the portion of the data corresponding to the top panel.

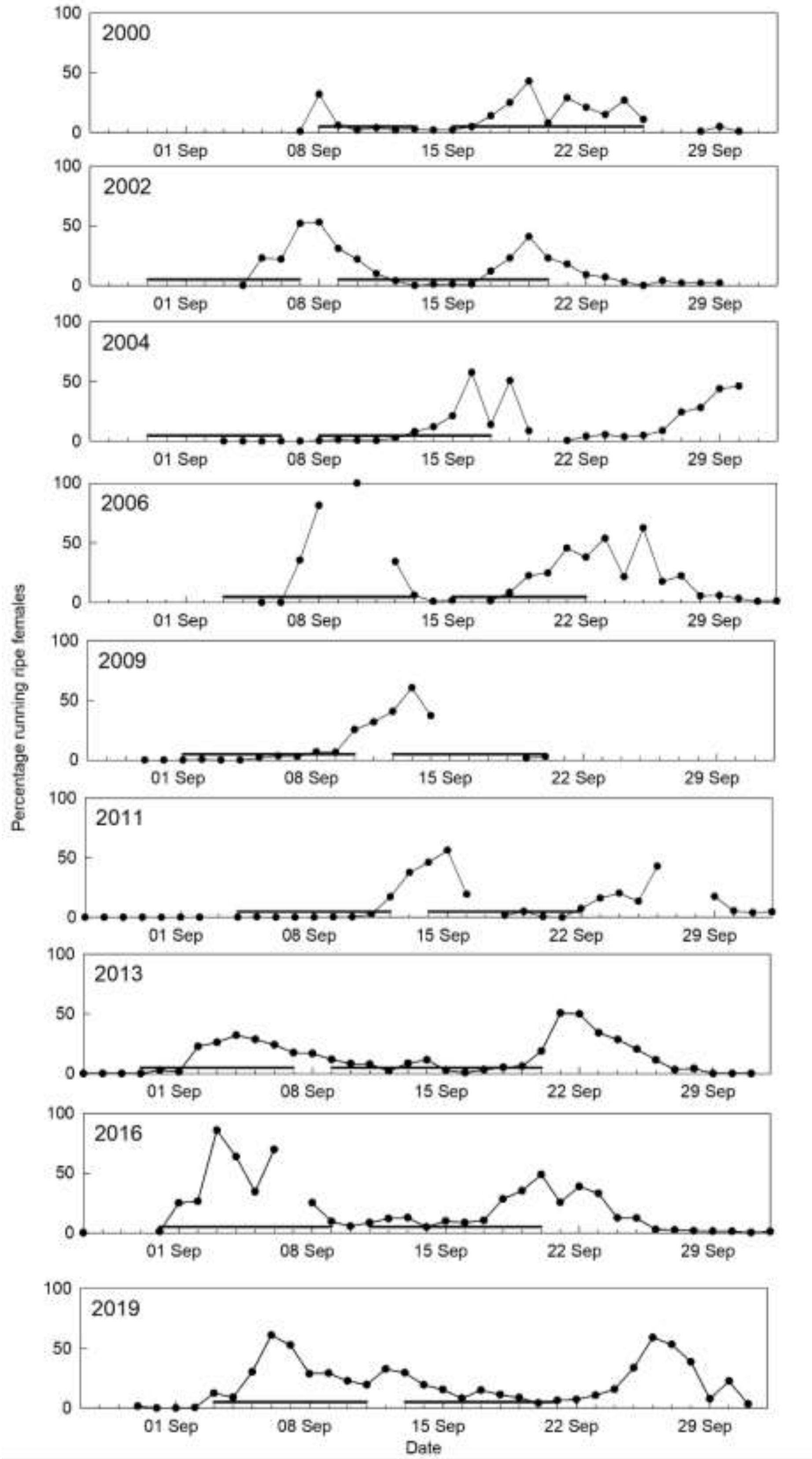

Figure 7: Survey timing (line above x axis) in relation to the timing of spawning for the acoustic surveys from 2000 to 2019 on the Campbell Island Rise. Percentage of running ripe females is from observer data.

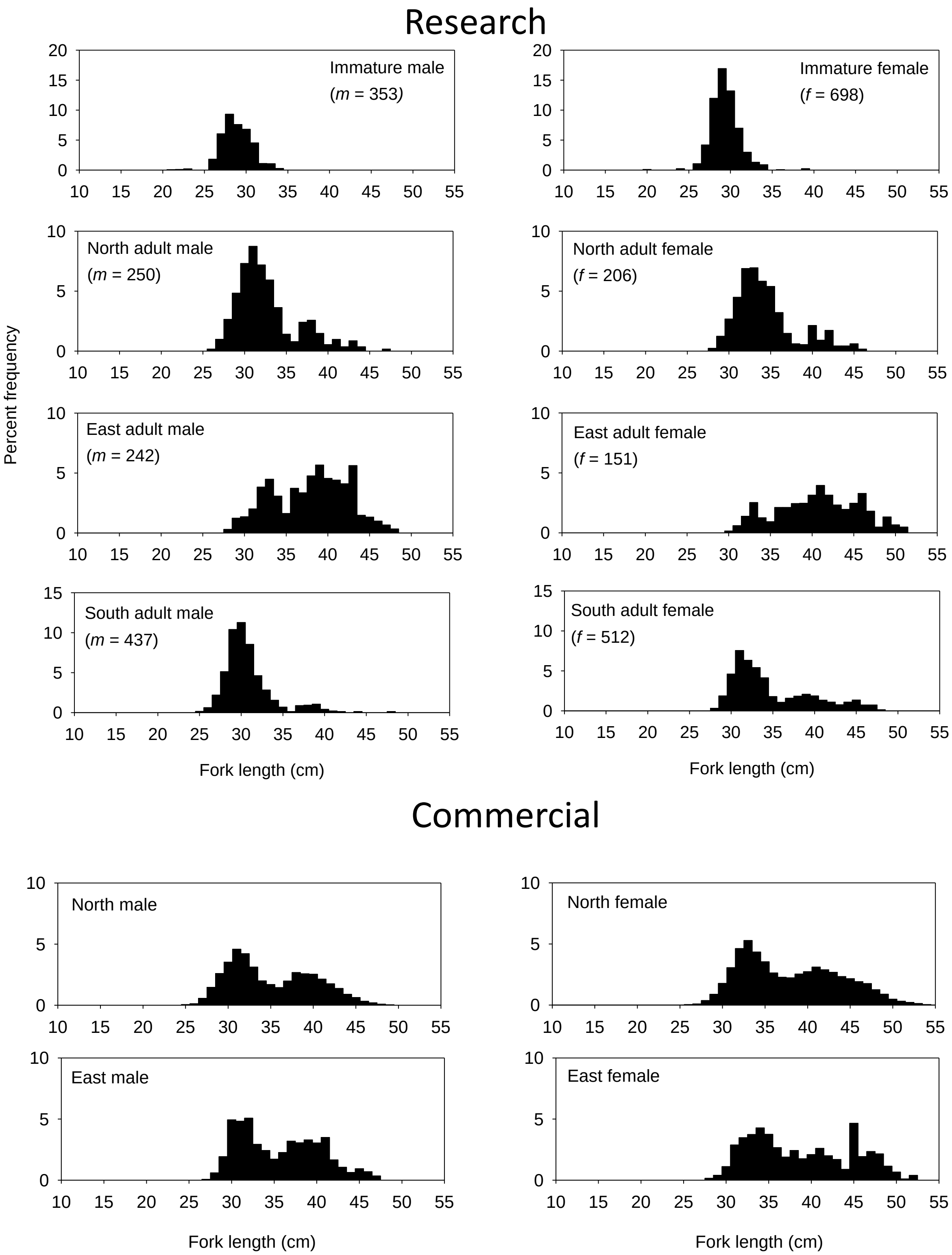

Figure 8: Catch-weighted length frequency distributions for southern blue whiting caught in research trawls during the 2019 acoustic survey (top panels), and from commercial tows during the spawning fishery (bottom panels). SBW are separated as immature or adult in research trawls. For adults, size distributions were separated into North (strata 2, 3N, 3S, 4, 5), East (strata 6N, 6S, 62, 8N, 8S, 8E, and 82), and South (strata 7N, 7S, 7S2). The m and f values for research trawls show number of males and females measured. No commercial tows were done in the southern area.

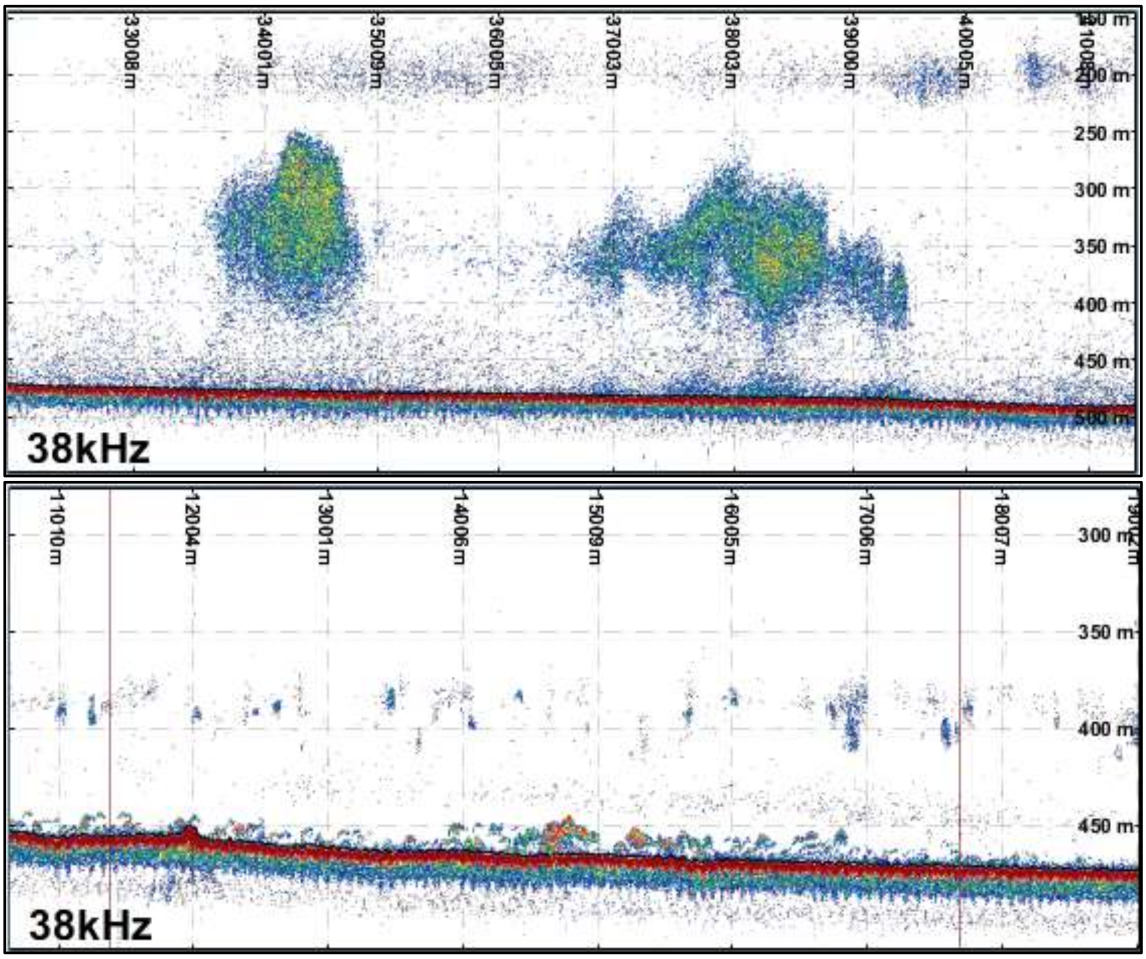

Figure 9: Example echograms showing marks of the northern aggregation of spawning adult SBW during snapshot 1 (top: transect 1 stratum 4, night; bottom: transect 3 stratum 4, day). Grid lines are every 1000 m horizontally and 50 m vertically. Vertical red lines are pings that have been flagged as "bad transmit" during grooming.

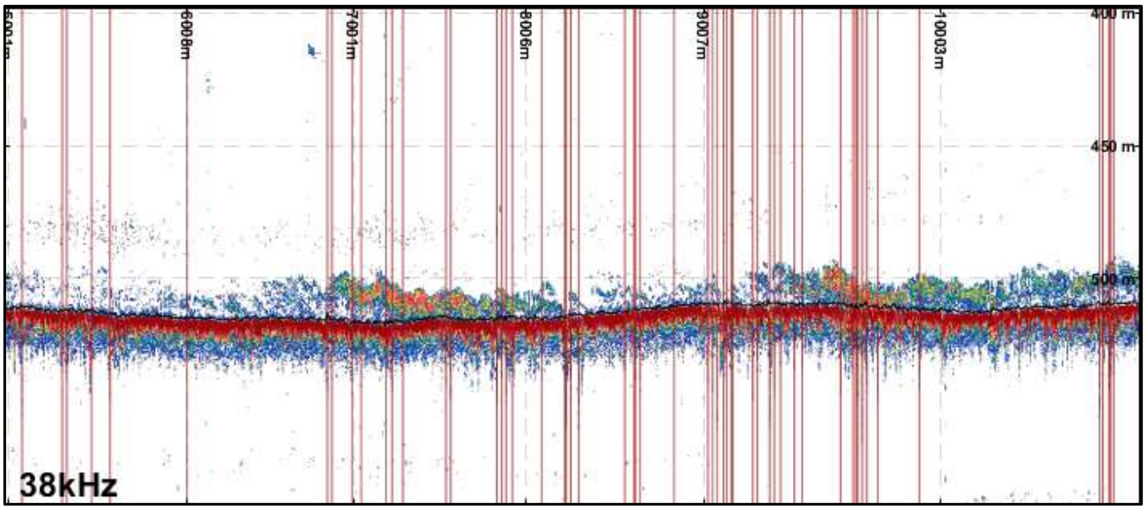

Figure 10: Example echogram showing marks of the eastern aggregation of post-spawning, dispersed adult SBW during snapshot 1 (transect 3 stratum 8S, day). Grid lines are every 1000 m horizontally and 50 m vertically. Vertical red lines are pings that have been flagged as "bad transmit" during grooming.

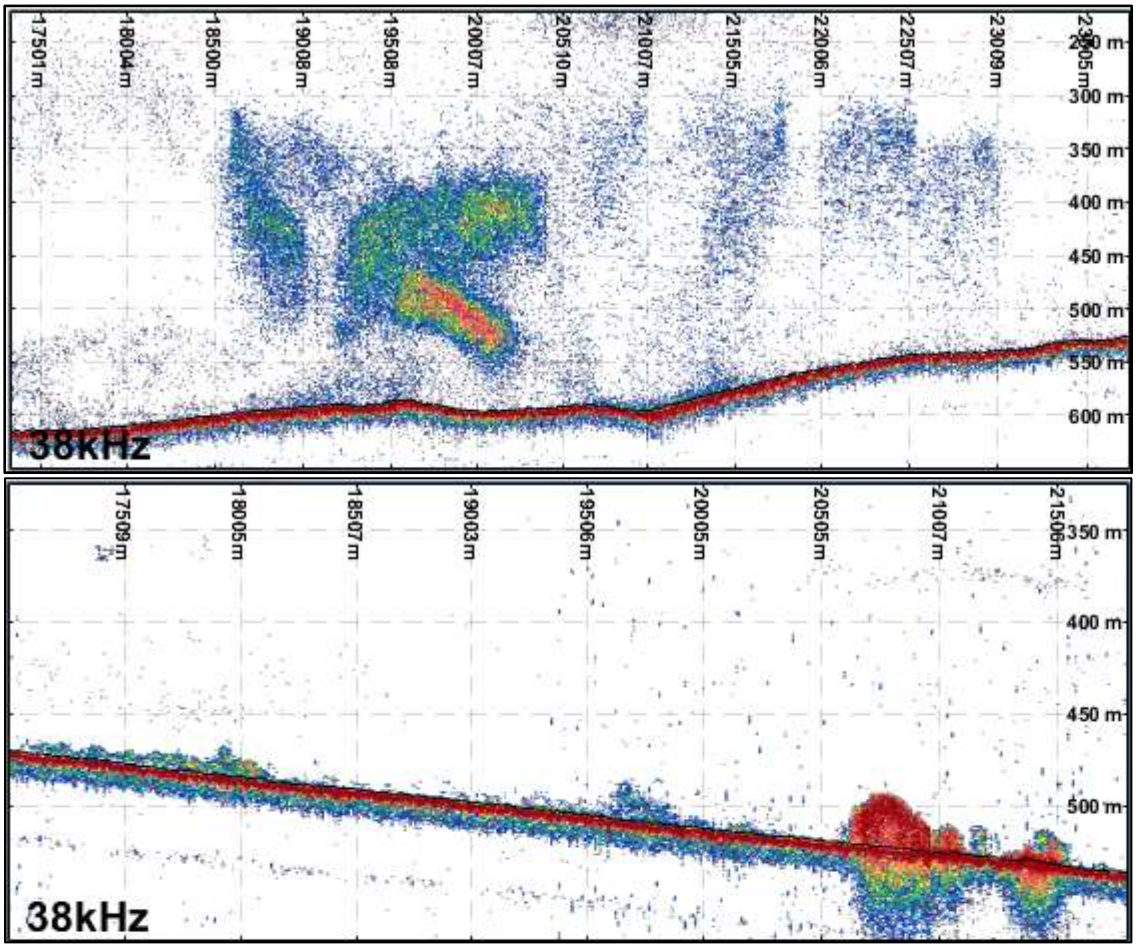

Figure 11: Example echograms showing marks of the southern aggregation of spawning adult SBW during snapshot 1 (top: transect 4 stratum 7S, night; bottom: transect 3 stratum 7S, day). Grid lines are every 1000 m horizontally and 50 m vertically.

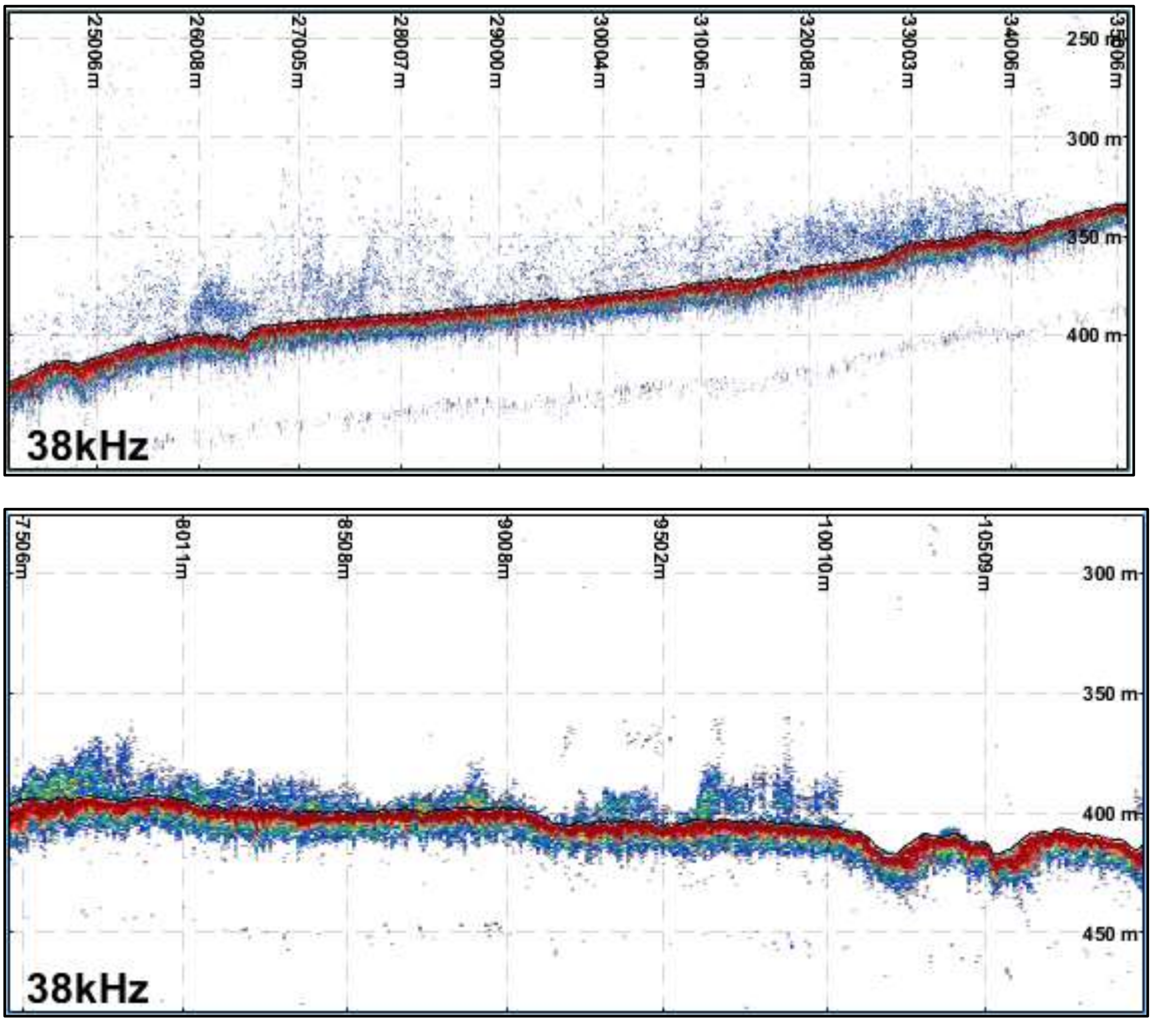

Figure 12: Example echograms showing marks of immature SBW (top: snapshot 1 transect 3 stratum 2, night; bottom: snapshot 2 transect 1 stratum 7S2, day). Grid lines are every 1000 m horizontally and 50 m vertically.

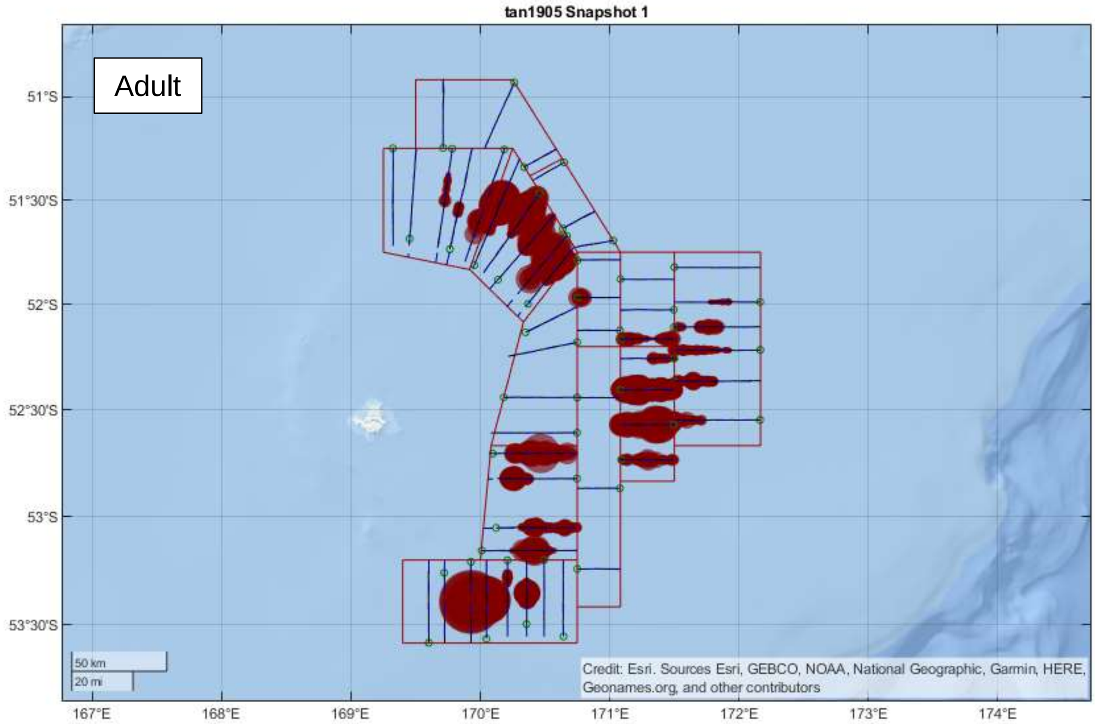

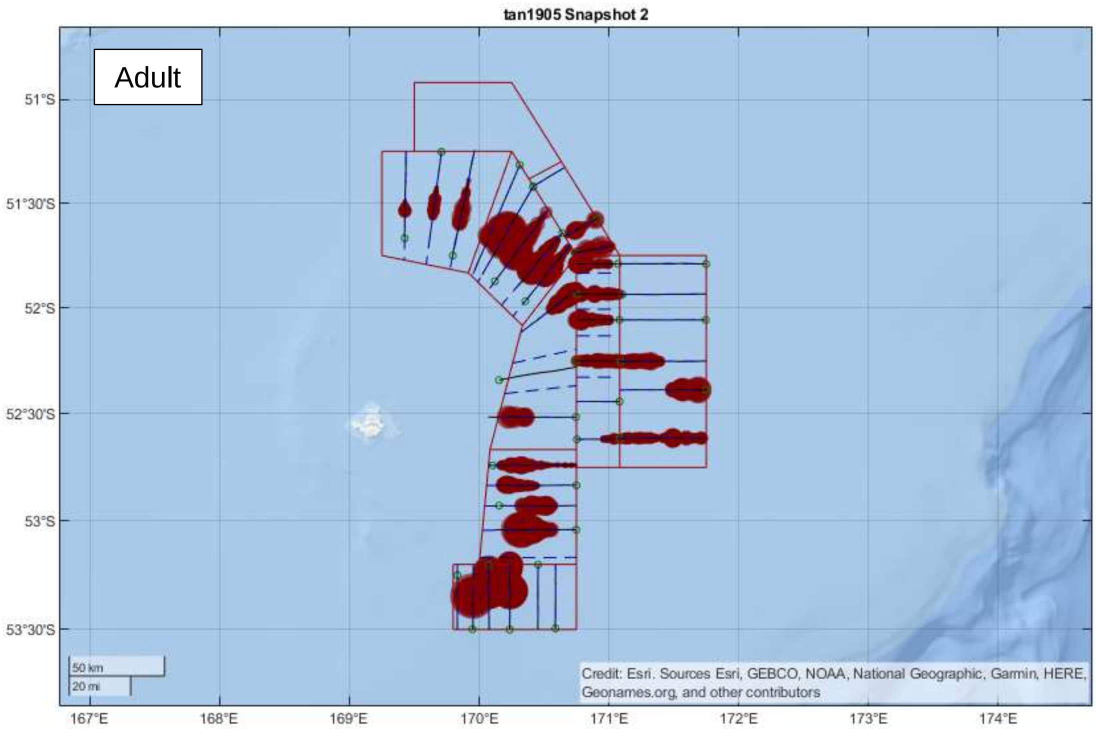

Figure 13: Spatial distribution of acoustic backscatter from adult SBW (averaged over 10 consecutive pings, i.e., approximately 100 m) for snapshots 1 (top) and 2 (bottom). Circle area is proportional to the log of the acoustic backscatter.

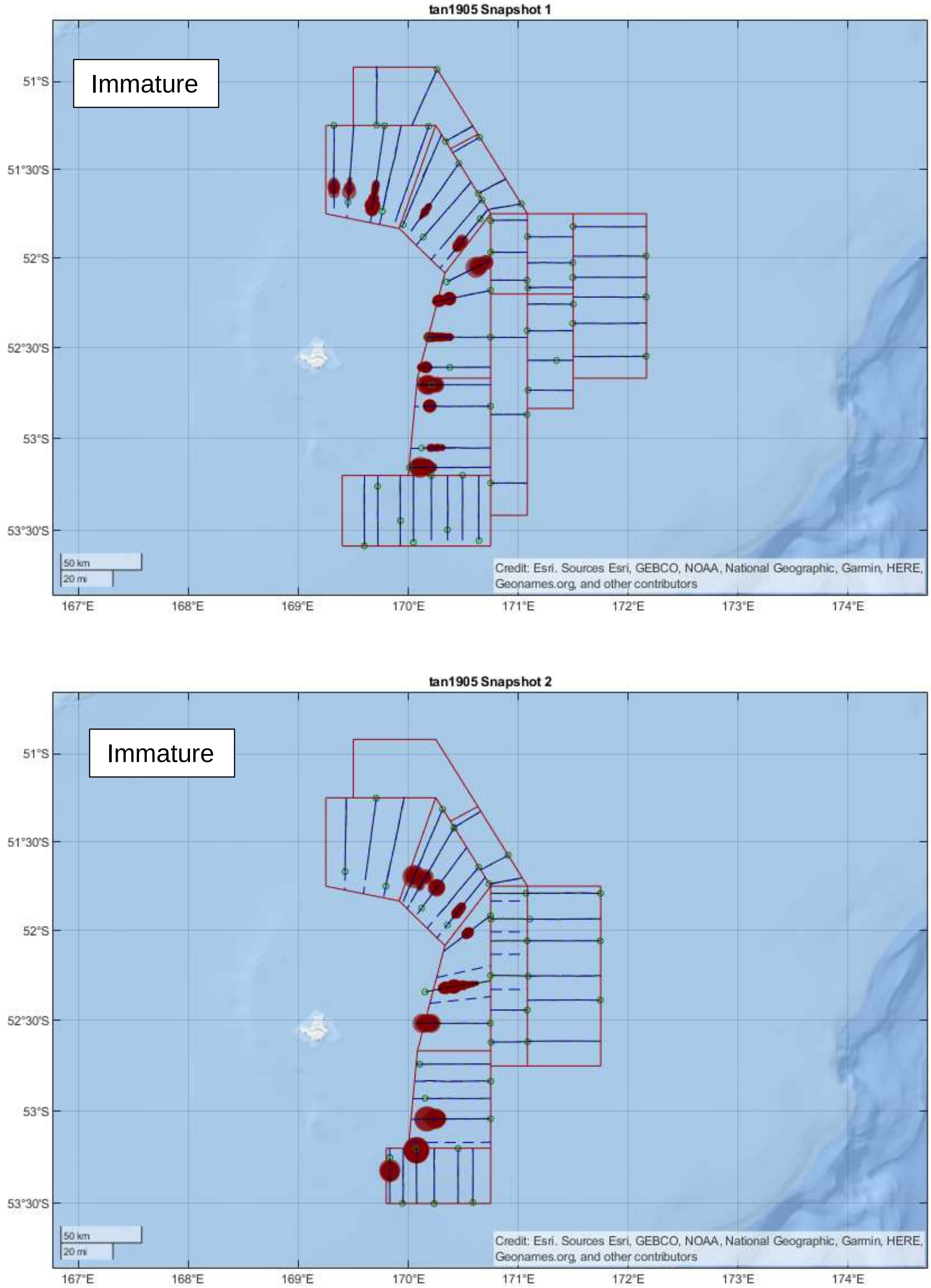

Figure 14: Spatial distribution of acoustic backscatter from immature SBW (averaged over 10 consecutive pings, i.e., approximately 100 m) for snapshots 1 (top) and 2 (bottom). Circle area is proportional to the log of the acoustic backscatter.

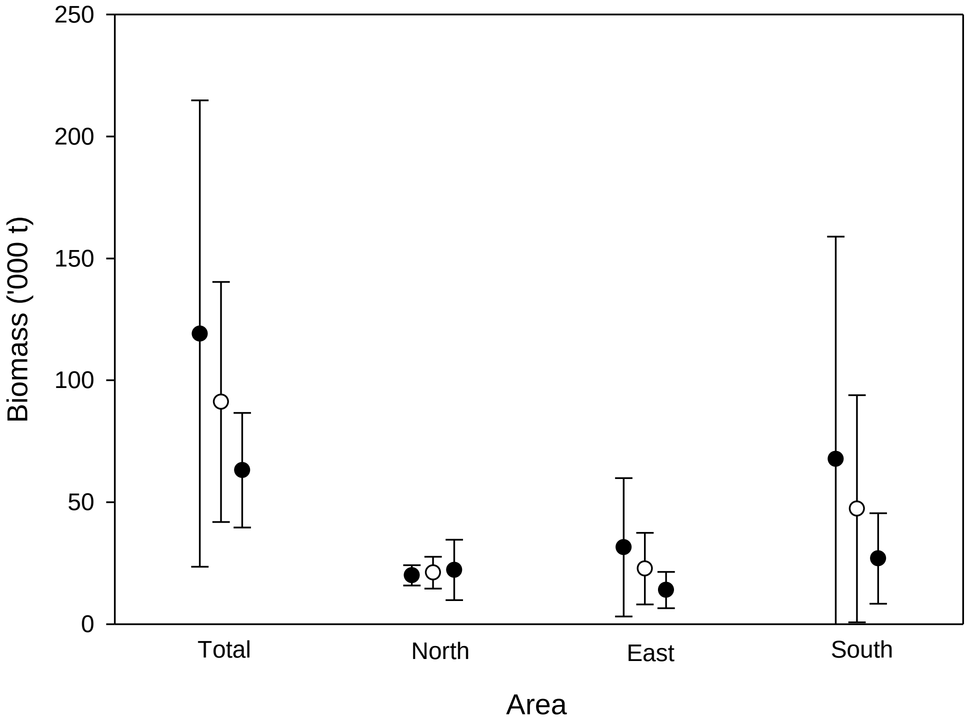

Figure 15: Comparison of snapshot 1 and 2 biomass estimates (in black) and their average (in white) for adult SBW, categorised by general area, for the 2019 Campbell acoustic survey. Error bars are ± 2 standard errors.

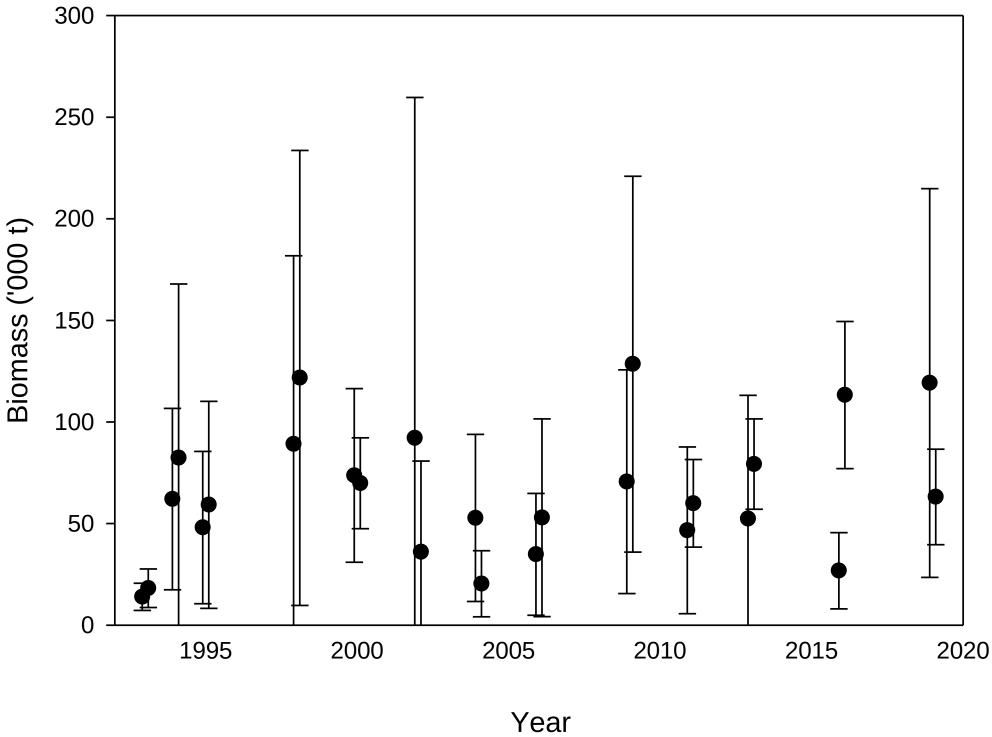

Figure 16: Comparison of snapshot 1 and 2 biomass estimates for adult SBW for all Campbell acoustic surveys. Error bars are ± 2 standard errors. Values for surveys from 1993–2011 are from Fu et al. (2013) and all were calculated using estimates of TS from O'Driscoll et al. (2013).

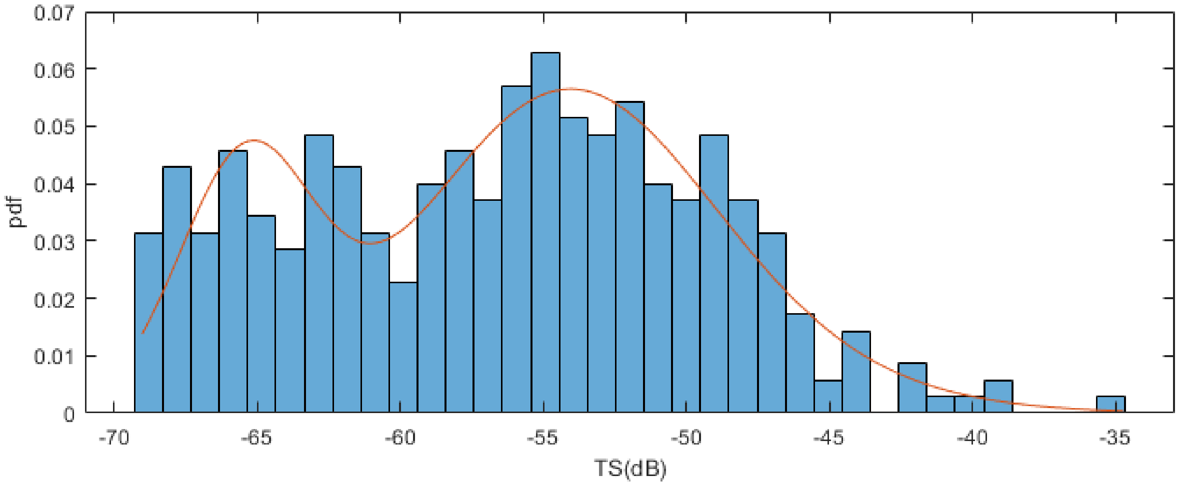

Figure 17: Probability density function of the mean TS of tracked targets during the AOS deployment on the trawl (station 8).

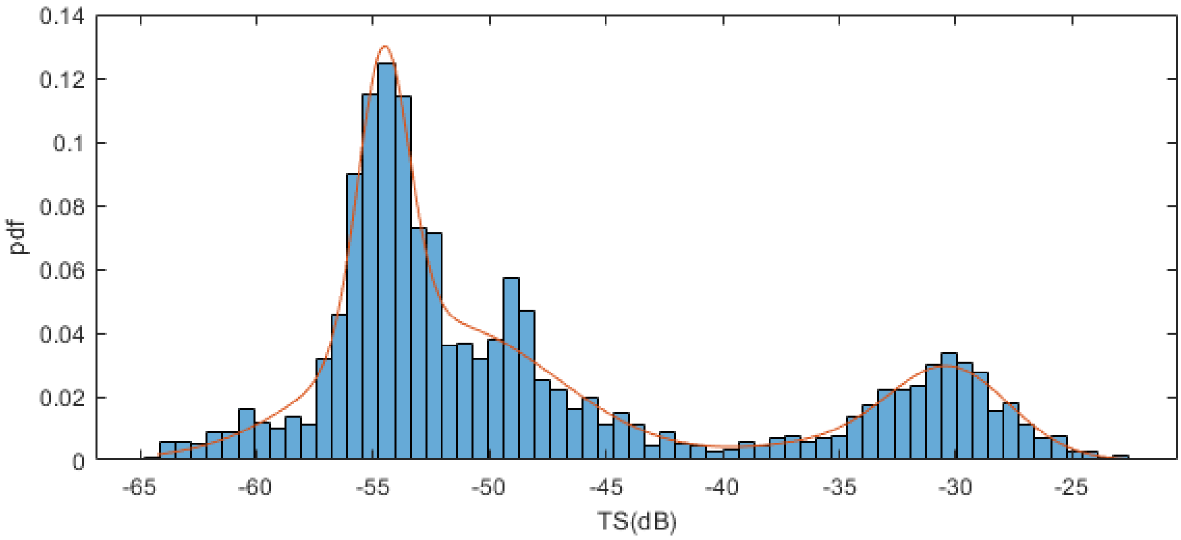

Figure 18: Probability density function of the mean TS of tracked targets during the AOS deployment in TS-probe mode (station 18). The orange curve is a 4 components Gaussian mixture model: Component 1, proportion 52%, mean -52.0 dB; Component 2, proportion 5%, mean -35.2 dB; Component 3, proportion 25%, mean -54.5 dB; Component 4, proportion 18%, mean -30.2 dB).

APPENDIX 1: Calibration of *Tangaroa* hull echosounders

The 18, 38, 70, 120, and 200 kHz EK60 echosounders on *Tangaroa* were calibrated on 30 August 2019 in Resolution Bay, Marlborough Sounds (41° 07.6' S, 174° 13.6' E), at the start of the Campbell southern blue whiting acoustic survey (TAN1905). The calibration was conducted broadly as per the procedures given by Demer et al. (2015).

New Zealand Diving Services provided SCUBA divers from their vessel *Topside*. The calibration started at 10:30 NZST. The sphere and associated lines were immersed in a soap solution prior to entering the water. A lead weight was also deployed about 3 m below the sphere to steady the arrangement of lines. The divers attached the lines and made sure these were not fouled. Long (3.4 m) fibreglass calibration poles were used to help keep the calibration lines clear of the hull.

The weather during the calibration was good, with 10 knots of south-easterly wind, no swell, and a 0.3 m chop. The vessel was anchored to eliminate drift but was swinging around its anchor at 0.3–0.5 knots. Water depth was about 41 m below the transducers.

The sphere was located in the beam immediately at 10:47, and the divers and support boat returned to port at 11:20. The sphere was first centred in the beam of the 38 kHz transducer to obtain data for the on-axis calibration. It was then moved around to obtain data for the beam shape calibration. Due to the proximity of all five transducers, several echoes were recorded across all frequencies. After the 38 kHz calibration, the sphere was moved to ensure on-axis calibration of the other frequencies.

The calibration data were recorded in one EK60 .raw format file (tan1905-D20190829-T224755.raw). These data are stored on the acoustic data server Odin, at NIWA. The transceiver settings in effect during the calibration are given in Table A1.1.

A temperature/salinity/depth profile was taken using a Seabird SBE21 CTD probe (serial number 2958). Estimates of acoustic absorption were calculated using the formulae of Doonan et al. (2003) for 18, 38, 70, and 120 kHz and the formula of Francois & Garrison (1982) for 200 kHz. Estimates of seawater sound speed and density were calculated using the formulae of Fofonoff & Millard (1983). The sphere target strength was calculated as per equations 6 to 9 given by MacLennan (1981) using longitudinal and transverse sphere sound velocities of 6853 and 4171 m s^{-1} respectively and a sphere density of 14 900 kg m^{-3}.

Analysis

The data in the raw EK60 file were extracted using the ESP3 software (version 1.4.1). The amplitude of the sphere echoes was obtained by filtering on range and choosing the sample with the highest amplitude. Instances where the sphere echo was disturbed by fish echoes were discarded. The alongship and athwartship beam widths and offsets were calculated by fitting the sphere echo amplitudes to the Simrad theoretical beam pattern:

$$compensation = 6.0206\left(\left(\frac{2\theta_{fa}}{BW_{fa}}\right)^2 + \left(\frac{2\theta_{ps}}{BW_{ps}}\right)^2 - 0.18\left(\frac{2\theta_{fa}}{BW_{fa}}\right)^2\left(\frac{2\theta_{ps}}{BW_{ps}}\right)^2\right), \quad \text{(A1.1)}$$

where θ_{ps} is the port/starboard echo angle, θ_{fa} the fore/aft echo angle, BW_{ps} the port/starboard beamwidth, BW_{fa} the fore/aft beamwidth, and *compensation* the value (in dB) to add to an uncompensated echo to yield the compensated echo value. The fitting was done using an unconstrained nonlinear optimisation (as implemented by the Matlab "fminsearch" function). The S_a correction was calculated from:

$$Sa,corr = 5\log 10\left(\frac{\sum P_i}{4P_{\max}}\right), \qquad (A1.2)$$

where P_i are the sphere echo power measurements and P_{max} the maximum sphere echo power measurement. A value for $S_{a,corr}$ is calculated for all valid sphere echoes and the mean over all sphere echoes is used to determine the final $S_{a,corr}$.

Results

The results from the CTD cast are given in Table A1.2, along with estimates of the sphere target strength, sound speed, and acoustic absorption for 18, 38, 70, 120, and 200 kHz.

The calibration parameters resulting from the calibration data analysis are given in Table A1.3 and compared with results from previous calibrations. Results for all frequencies have been relatively consistent (usually within 0.5 dB) across all calibrations, with higher frequencies (especially the 120 kHz) being more variable over time. The G_0 for the 120 kHz transducer was 0.42 dB higher in this calibration than that from the previous calibration in January 2019, but within the range of values since 2012.

In January 2019, the G_0 for the 18 kHz transducer was 0.63 dB higher than the previous calibration in August 2016. There was a concern that an event in July 2018 (the 18 kHz transducer was used in broadband mode connected to a WBT) may have impacted the physical characteristics of the transducer. However, the G_0 for the 18 kHz transducer for this new calibration is 0.51 dB lower than the January 2019 calibration and similar to the previous calibrations (2012–16), which suggests the transducer is operating normally. The new 38 kHz transducer (installed in October 2015) has slightly higher estimated gain than the previous transducer, but has been stable, with very similar estimated calibration parameters in its five calibrations.

The estimated beam patterns, as well as the coverage of the beam by the calibration sphere, are given in Figures A1.1–A1.10. The symmetrical nature of the beam patterns and the centering near zero indicates that the transducers and EK60 transceivers were all operating correctly.

The root mean square (RMS) of the difference between the Simrad beam model and the sphere echoes out to the 3 dB beamwidth was 0.08 dB for 18 kHz, 0.08 for 38 kHz, 0.06 dB for 70 kHz, 0.17 dB for 120 kHz, and 0.20 dB at 200 kHz (Table A1.3), indicating excellent quality calibrations on all frequencies (values <0.2 dB are excellent). On-axis estimates were derived from 279 sphere echoes at 18 kHz, 436 echoes at 38 kHz, 346 echoes at 70 kHz, 142 echoes at 120 kHz, and 27 echoes at 200 kHz.

Table A1.1: EK60 transceiver settings and other relevant parameters in effect during the calibration.

Parameter					
Frequency (kHz)	18	38	70	120	200
GPT model	00907205c476	0090720580ea	00907205ca98	009072058148	00907205da23
GPT serial number	652	650	674	668	692
GPT software version	070413	070413	070413	070413	070413
EK80 software version	1.12.2	1.12.2	1.12.2	1.12.2	1.12.2
Transducer model	ES18-11	ES38B	ES70-7C	ES120-7C	ES200-7C
Transducer serial number	2080	31378	158	477	364
Sphere type/size	tungsten carbide (38.1 mm diameter)				
Transducer draft setting (m)	0.0	0.0	0.0	0.0	0.0
Transmit power (W)	2000	2000	750*	250*	150*
Pulse length (ms)	1.024	1.024	1.024	1.024	1.024
Transducer peak gain (dB)	22.40	25.50	27.00	27.00	27.00
Sa correction (dB)	0.00	0.00	0.00	0.00	0.00
Sample interval (ms)	0.256	0.256	0.256	0.256	0.256
Two-way beam angle (dB)	–17.0	–20.7	–20.7	–20.7	–20.7
Angle sensitivity (dB) along/athwartship	15.5/15.5	23.0/23.0	23.0/23.0	23.0/23.0	23.0/23.0
3 dB beamwidth (º) along/athwartship	11.0/11.0	7.0/7.0	7.0/7.0	7.0/7.0	7.0/7.0
Angle offset (º) along/athwartship	0.0/0.0	0.0/0.0	0.0/0.0	0.0/0.0	0.0/0.0
Sound speed (m/s)	1500	1500	1500	1500	1500
Absorption (dB/km)	3.0	10.0	23.0	38.0	54.0

* Prior to 2013, transmit power for 70, 120, and 200 kHz was 1000, 500, and 300 W respectively.

Table A1.2: CTD cast details and derived water properties. The values for sound speed, salinity and absorption are the mean over water depths 6 to 30 m.

Parameter	
Date/time (NZST, start)	30 Aug 2019 13:56
Position	41° 07.58’ S, 174° 13.59’ E
Mean sphere range (m)	24.1 (18 kHz), 24.0 (38), 24.0 (70), 23.9 (120), 15.3 (200)
Mean temperature (ºC)	12.1
Mean salinity (psu)	34.7
Sound speed (m/s)	1497
Water density (kg/m^3)	1026.4
Sound absorption (dB/km)	2.34 (18 kHz) 9.16 (38 kHz) 22.67 (70 kHz) 39.26 (120 kHz) 58.51 (200 kHz)
Sphere target strength (dB re 1m^2)	–42.64 (18 kHz) –42.41 (38 kHz) –41.40 (70 kHz) –39.51 (120 kHz) –39.10 (200 kHz)

Table A1.3: Estimated calibration coefficients for all calibrations of *Tangaroa* hull EK60 echosounders since 2012. Transducer peak gain was estimated from mean sphere TS. [Continued on the next page]

	Aug 2019	Jan 2019**	Jul 2018	Aug 2016	Feb 2016	Feb 2015**	Jul 2013	Jul 2012	Feb 2012
18 kHz									
Transducer peak gain (dB)	22.92	23.43	N/A	22.80	22.85	23.21	22.99	22.97	22.81
Sa correction (dB)	-0.79	-0.76	N/A	-0.71	-0.73	-0.76	-0.78	-0.84	-0.69
Beamwidth (º) along/athwartship	9.8/10.0	9.7/9.7	N/A	10.6/10.9	10.5/11.3	10.7/11.2	10.6/10.7	10.7/11.2	10.7/10.9
Beam offset (º) along/athwartship	-0.04/0.12	-0.04/0.14	N/A	0.00/0.00	0.00/0.00	0.00/0.00	0.00/-0.00	0.00/-0.00	0.00/-0/.00
RMS deviation (dB)	0.08	0.12	N/A	0.10	0.14	0.12	0.08	0.09	0.14
38 kHz*									
Transducer peak gain (dB)	26.31	26.32	26.37	26.23	26.21	25.69	25.42	25.62	25.75
Sa correction (dB)	-0.59	-0.56	-0.55	-0.62	-0.58	-0.54	-0.55	-0.61	-0.57
Beamwidth (º) along/athwartship	6.8/6.8	6.6/6.6	6.7/6.8	7.0/7.1	6.9/7.2	6.8/6.9	6.8/6.9	6.8/6.9	6.8/6.8
Beam offset (º) along/athwartship	0.06/-0.12	0.11/-0.14	0.06/-0.08	0.00/0.00	0.14/-0.19	0.00/0.00	0.00/0.00	0.00/0.00	0.00/0.00
RMS deviation (dB)	0.08	0.14	0.12	0.11	0.14	0.12	0.09	0.10	0.14
70 kHz									
Transducer peak gain (dB)	26.36	26.27	N/A	26.33	26.28	26.55	26.43	26.04	26.78
Sa correction (dB)	-0.33	-0.32	N/A	-0.31	-0.38	-0.35	-0.37	-0.31	-0.35
Beamwidth (º) along/athwartship	6.8/6.8	6.4/6.5	N/A	6.4/6.6	6.2/6.5	6.6/6.7	6.6/6.3	6.6/6.6	6.3/6.1
Beam offset (º) along/athwartship	0.00/0.00	0.02/0.06	N/A	0.00/0.00	0.13/-0.04	0.04/-0.02	0.00/0.00	0.00/0.00	0.00/0.00
RMS deviation (dB)	0.06	0.16	N/A	0.13	0.18	0.10	0.10	0.10	0.21
120 kHz									
Transducer peak gain (dB)	26.71	26.29	26.20	26.19	26.15	26.92	26.22	26.11	26.80
Sa correction (dB)	-0.38	-0.37	-0.45	-0.33	-0.29	-0.33	-0.39	-0.34	-0.38
Beamwidth (º) along/athwartship	6.5/6.4	6.4/6.6	67/6.8	6.3/6.5	6.1/6.2	6.4/6.5	6.5/6.4	6.5/6.6	6.0/6.0
Beam offset (º) along/athwartship	-0.10/0.04	-0.01/-0.01	-0.02/0.00	0.00/0.00	-0.00/0.00	-0.00/0.00	0.00/0.00	-0.00/-0.00	0.00/0.00
RMS deviation (dB)	0.17	0.18	0.20	0.17	0.18	0.16	0.15	0.17	0.19

	Aug 2019	Jan 2019**	Jul 2018	Aug 2016	Feb 2016	Feb 2015**	Jul 2013	Jul 2012	Feb 2012
200 kHz									
Transducer peak gain (dB)	25.09	24.98	25.15	24.92	25.10	24.90	25.27	25.31	25.16
Sa correction (dB)	-0.33	-0.20	-0.29	-0.17	-0.22	-0.27	-0.31	-0.24	-0.21
Beamwidth (º) along/athwartship	6.8/6.6	6.3/6.4	6.5/6.5	6.4/6.3	6.2/6.2	6.6/6.9	6.4/6.3	6.8/6.5	6.2/6.2
Beam offset (º) along/athwartship	-0.24/-0.08	0.18/-0.08	-0.03/-0.1	0.00/0.00	0.00/0.00	0.00/0.00	0.00/0.00	-0.27/-0.10	0.08/-0.08
RMS deviation (dB)	0.20	0.19	0.25	0.19	0.18	0.20	0.20	0.21	0.18

* The 38 kHz transducer was changed in October 2015.
** The Jan 2019 and Feb 2015 calibrations were in Antarctica.

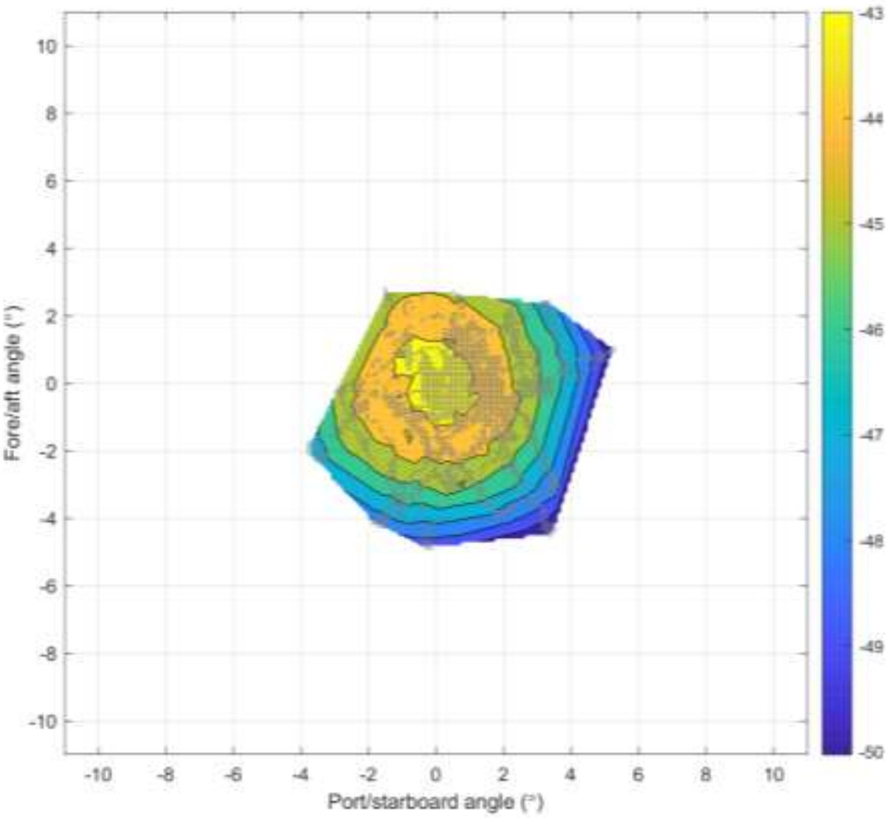

Figure A1.1: The 18 kHz estimated beam pattern from the sphere echo strength and position. The '+' symbols indicate where sphere echoes were received. The colours indicate the received sphere echo strength in dB re 1 m^2.

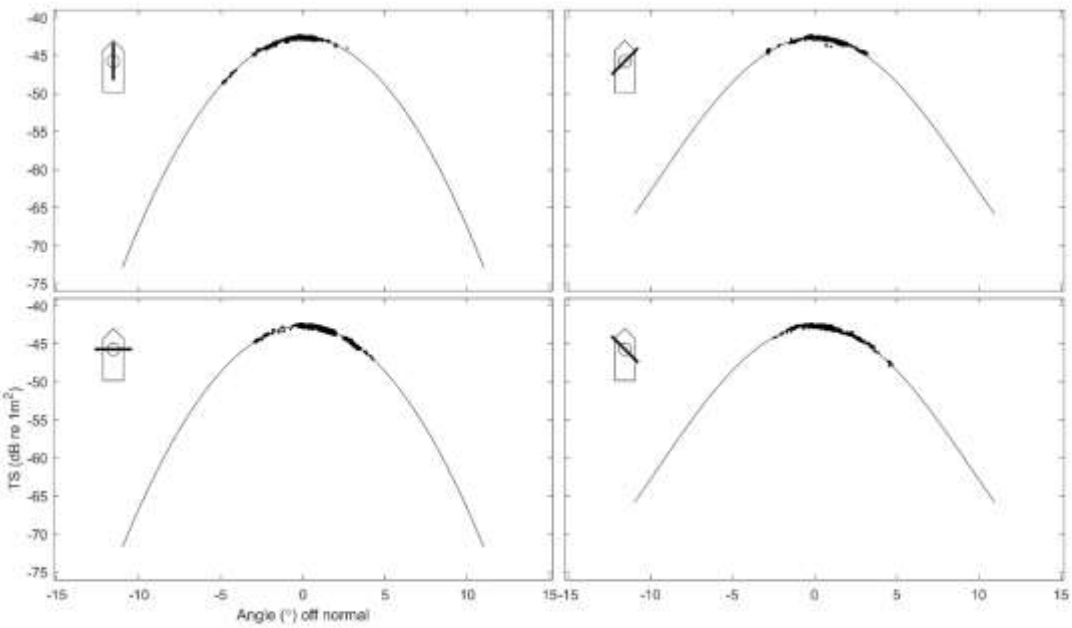

Figure A1.2: Beam pattern results from the 18 kHz analysis. The solid line is the ideal beam pattern fit to the sphere echoes for four slices through the beam.

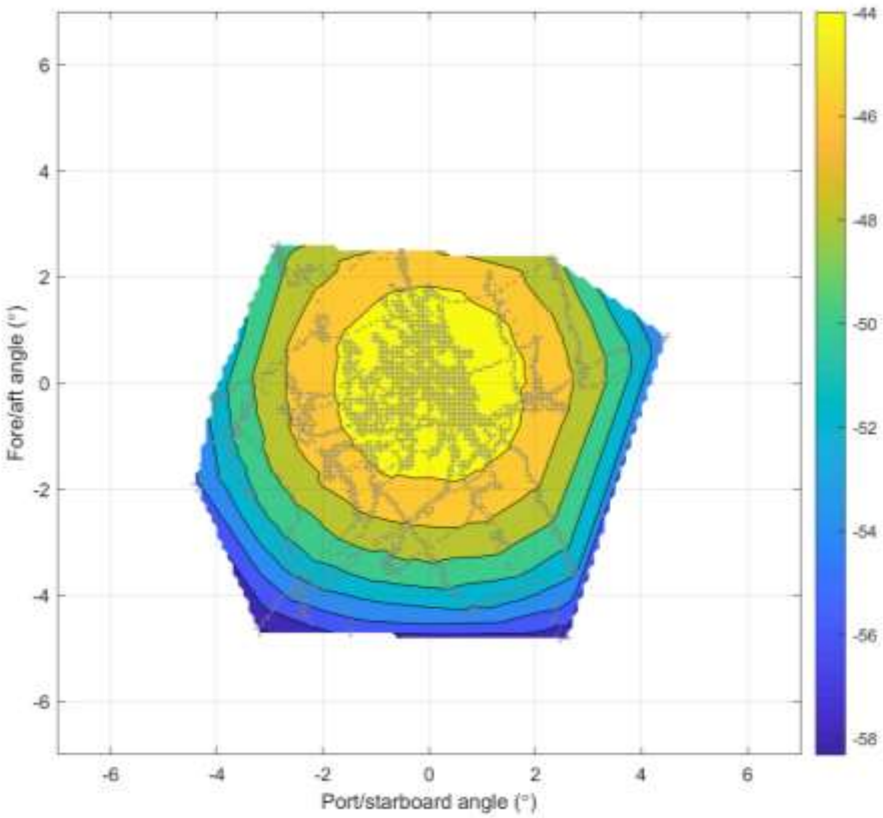

Figure A1.3: The 38 kHz estimated beam pattern from the sphere echo strength and position. The '+' symbols indicate where sphere echoes were received. The colours indicate the received sphere echo strength in dB re 1 m^2.

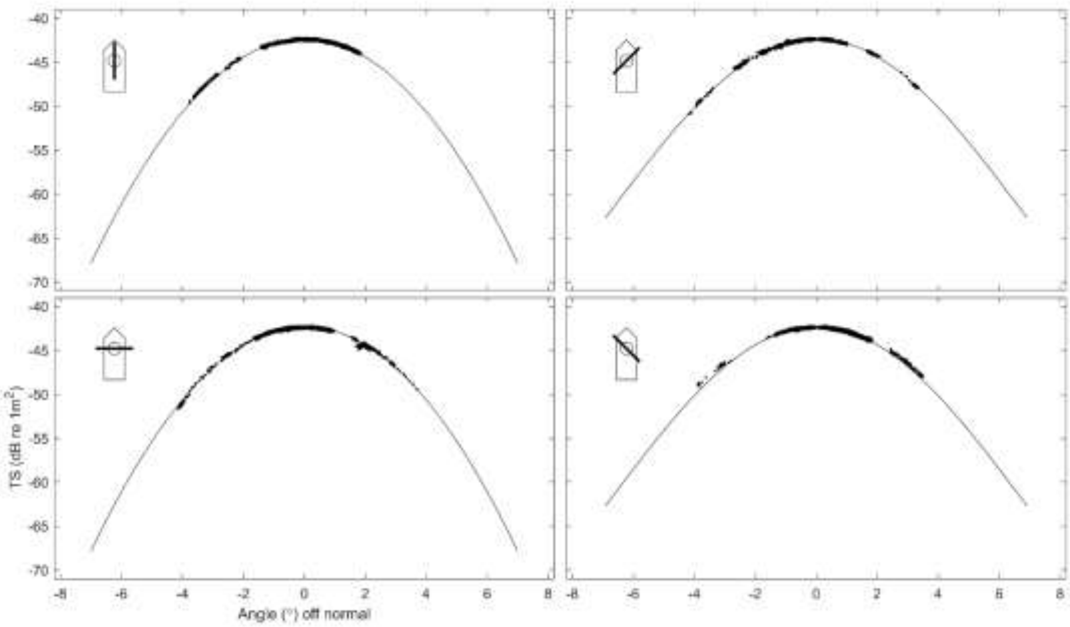

Figure A1.4: Beam pattern results from the 38 kHz analysis. The solid line is the ideal beam pattern fit to the sphere echoes for four slices through the beam.

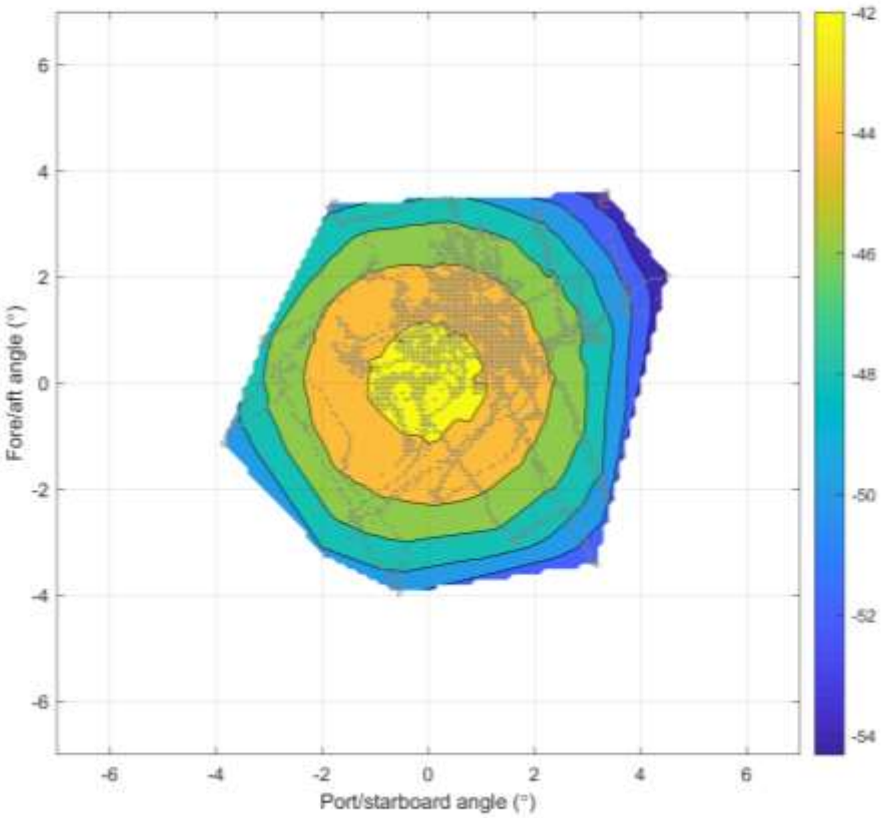

Figure A1.5: The 70 kHz estimated beam pattern from the sphere echo strength and position. The '+' symbols indicate where sphere echoes were received. The colours indicate the received sphere echo strength in dB re 1 m^2.

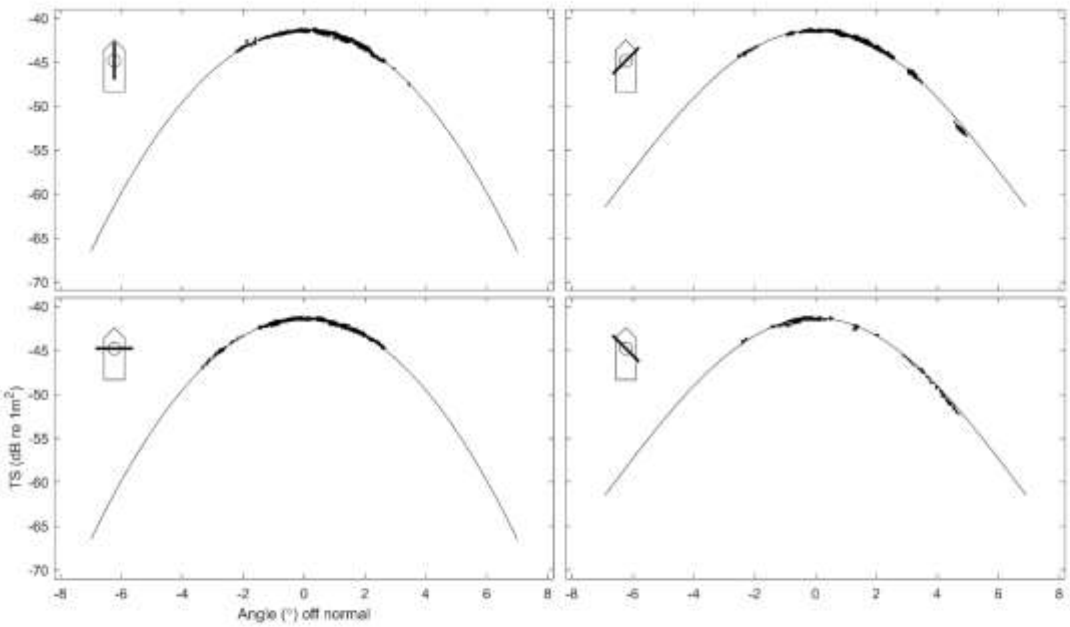

Figure A1.6: Beam pattern results from the 70 kHz analysis. The solid line is the ideal beam pattern fit to the sphere echoes for four slices through the beam.

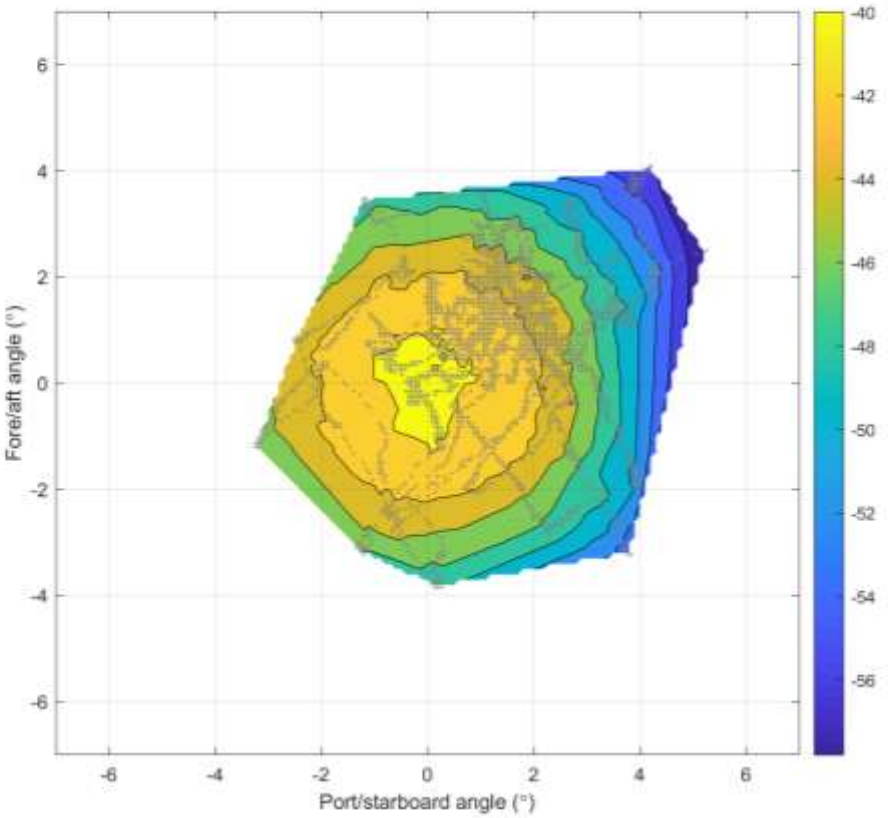

Figure A1.7: The 120 kHz estimated beam pattern from the sphere echo strength and position. The '+' symbols indicate where sphere echoes were received. The colours indicate the received sphere echo strength in dB re 1 m^2.

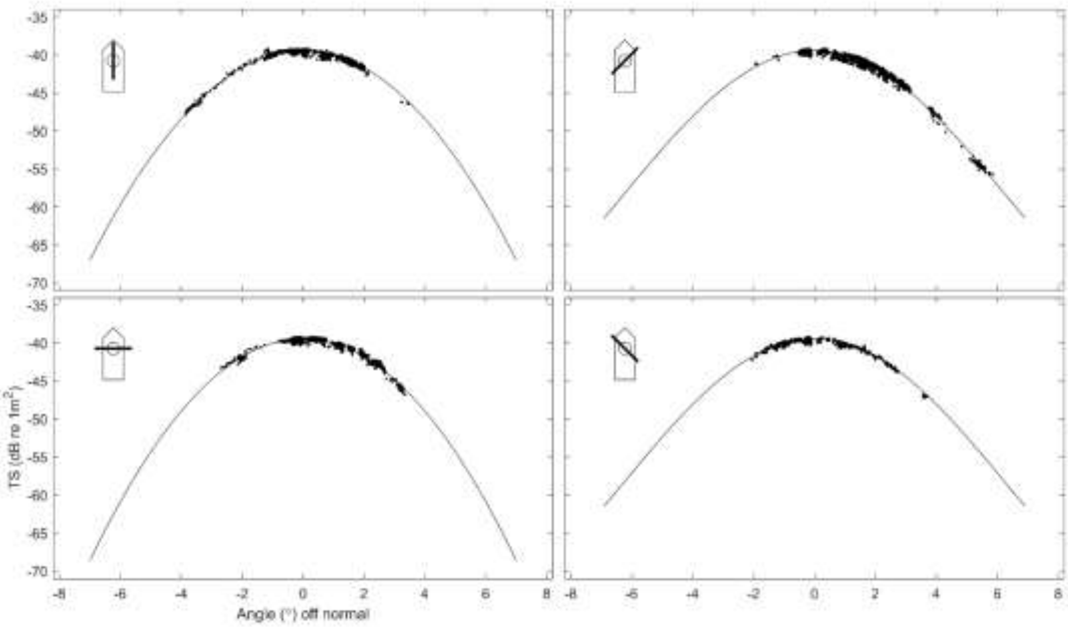

Figure A1.8: Beam pattern results from the 120 kHz analysis. The solid line is the ideal beam pattern fit to the sphere echoes for four slices through the beam.

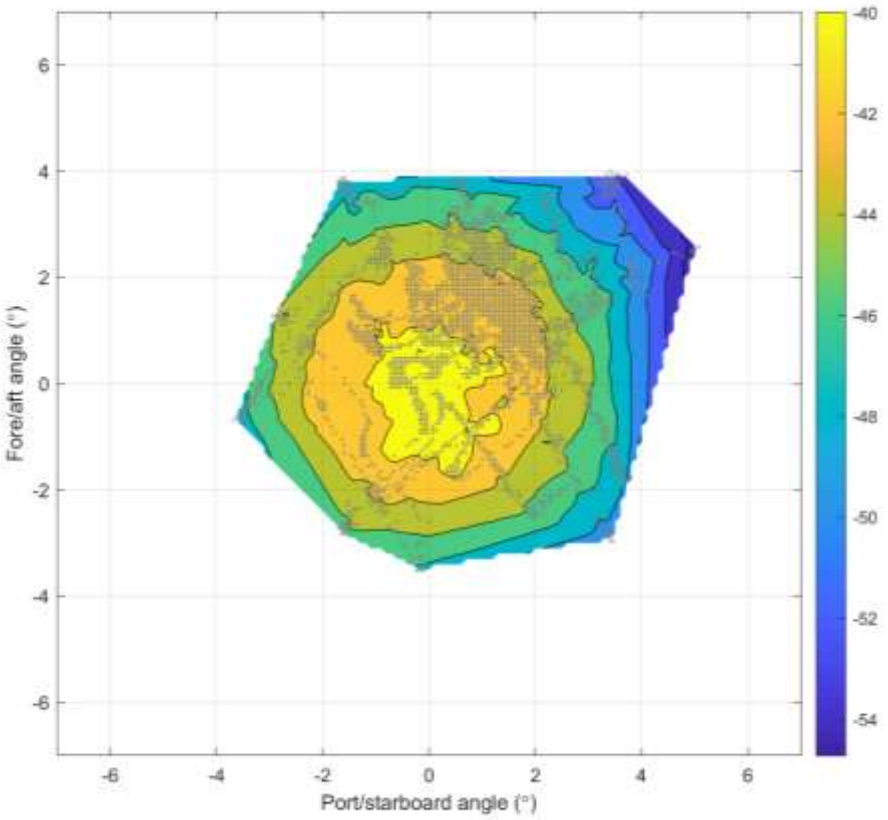

Figure A1.9: The 200 kHz estimated beam pattern from the sphere echo strength and position. The '+' symbols indicate where sphere echoes were received. The colours indicate the received sphere echo strength in dB re 1 m^2.

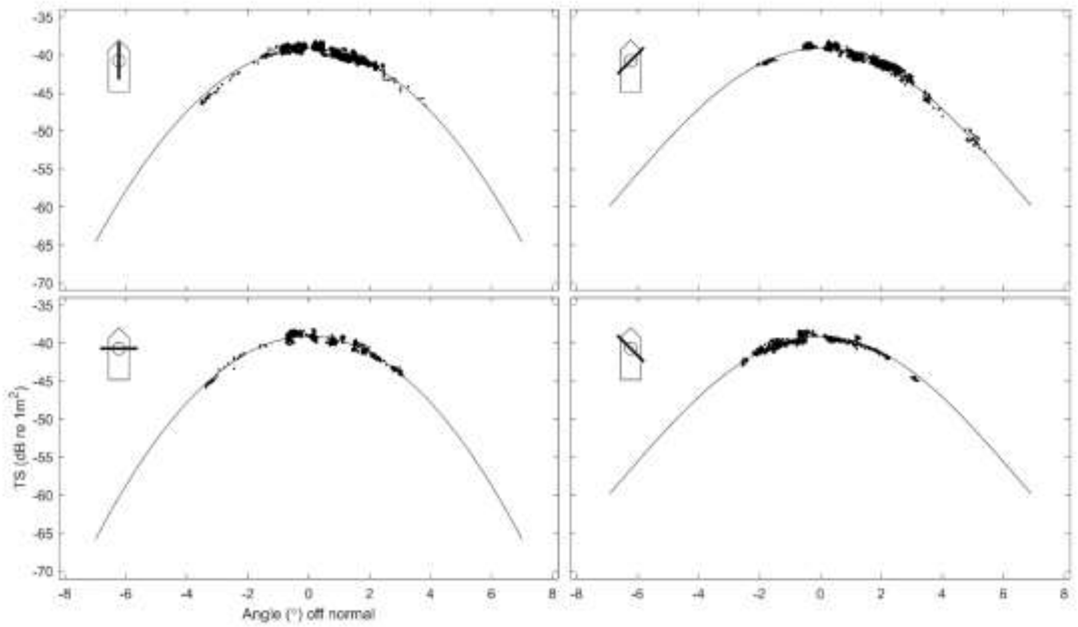

Figure A1.10: Beam pattern results from the 200 kHz analysis. The solid line is the ideal beam pattern fit to the sphere echoes for four slices through the beam.

APPENDIX 2: Towbody 4 calibration

Calibration of the Simrad EK60 echosounder in Towbody 4 took place on 30 August 2019 in Resolution Bay, Marlborough Sounds (41° 07.6' S, 174° 13.6' E), at the start of the Campbell southern blue whiting acoustic survey (TAN1905), and on 17 September 2019 in Perseverance Harbour, Campbell Island (52° 33.0' S, 169° 12.3' E) during the survey. The calibrations were conducted broadly as per the procedures given by Demer et al. (2015).

In both calibrations, the towbody was lowered about 3 m below the surface, supported by the deployment wires and a nose rope to allow the pitch to be adjusted. A 38.1 mm tungsten carbide sphere was suspended by a single line about 35 m below the transducer. A weight was also deployed about 3 m below the sphere to steady the line. The transducer face, towbody window, sphere, and associated lines were washed with a soap solution prior to entering the water.

In the Marlborough Sounds, the weather during the calibration was good, with 10 knots of south-easterly wind, no swell, and a 0.3 m chop. The vessel was anchored but swinging at 0.3-0.5 knots. Water depth was about 45 m. The towbody calibration started at 12:00 NZST and was completed at 13:36.

At Campbell Island, the weather was rough with a 30 knot south-westerly wind and 1.0 m wind chop. The vessel was anchored in 36 m of water but was swinging on the anchor at speeds up to 1.0 knots. Vessel motion was enough to move the towbody around the beam with little manipulation of the supporting lines. The calibration started at 11:17 and was completed at 13:32.

The echosounder was run from a PC (ER60-1) onboard *Tangaroa* and calibration data were saved into Simrad .raw format files (tan1905-D20190830-T000013, tan1905-D20190830-T001411, tan1905-D20190830-T003348, tan1905-D20190830-T004452, tan1905-D20190830-T011113 in the Marlborough Sounds, tan1905-D20190916-T231745 at Campbell Island). Raw data are stored on the acoustic data server Odin, at NIWA. The transceiver settings in effect during the calibration are given in Table A2.1.

Temperature/salinity/depth profiles were taken using a Seabird SBE21 CTD probe (serial number 2958) during both calibrations. Estimates of acoustic absorption were calculated using the formulae of Doonan et al. (2003). Estimates of seawater sound speed and density were calculated using the formulae of Fofonoff & Millard (1983). The sphere target strength was calculated as per equations 6 to 9 given by MacLennan (1981), using longitudinal and transverse sphere sound velocities of 6853 and 4171 m s^{-1} respectively and a sphere density of 14 900 kg m^{-3}.

Analysis

The data in the .raw files were extracted using the ESP3 software (version 1.4.1). The amplitude of the sphere echoes was obtained by filtering on range and choosing the sample with the highest amplitude. The filter parameter *maxbBDiff1* which discarded sphere echoes which differed by more than 6 dB from the theoretical before estimating beam fit was increased to 9 dB because Towbody 4 had very low values for sphere TS. Instances where the sphere echo was disturbed by fish echoes were discarded. The alongship and athwartship beam widths and offsets were calculated by fitting the sphere echo amplitudes to the Simrad theoretical beam pattern:

$$compensation = 6.0206\left(\left(\frac{2\theta_{fa}}{BW_{fa}}\right)^2 + \left(\frac{2\theta_{ps}}{BW_{ps}}\right)^2 - 0.18\left(\frac{2\theta_{fa}}{BW_{fa}}\right)^2\left(\frac{2\theta_{ps}}{BW_{ps}}\right)^2\right), \quad \text{(A2.1)}$$

where θ_{ps} is the port/starboard echo angle, θ_{fa} the fore/aft echo angle, BW_{ps} the port/starboard beamwidth, BW_{fa} the fore/aft beamwidth, and *compensation* the value, in dB, to add to an uncompensated echo to yield the compensated echo value. The fitting was done using an unconstrained nonlinear optimisation (as implemented by the Matlab "fminsearch" function). The S_a correction was calculated from:

$$Sa,corr = 5\log 10\left(\frac{\sum P_i}{4P_{\max}}\right), \qquad \text{(A2.2)}$$

where P_i are the sphere echo power measurements and P_{max} the maximum sphere echo power measurement. A value for $S_{a,corr}$ is calculated for all valid sphere echoes and the mean over all sphere echoes is used to determine the final $S_{a,corr}$.

Results

The results from the CTD casts are given in Table A2.2, along with estimates of the sphere target strength, sound speed, and acoustic absorption.

The calibration results are given in Table A2.3. The estimated beam pattern and sphere coverage are given in Figures A2.1–A2.2. The symmetrical nature of the pattern and the zero centre of the beam pattern indicate that the transducer and EK60 transceiver were operating correctly. The fits between the theoretical beam pattern and the sphere echoes is shown in Figures A2.3–A2.4 and confirm that the transducer beam pattern is correct.

The estimated peak gain (G_0) of 23.88 dB and the Sa correction of -0.55 dB in the Marlborough Sounds were estimated from 507 sphere echoes within 0.21° of the beam centre (Table A2.3). This calibration was of excellent quality. The RMS of the difference between the Simrad beam model and the sphere echoes the sphere echoes out to 3.6° off axis was 0.16 dB (where <0.2 dB is considered excellent). The calibration at Campbell Island gave very similar values, with an estimated G_0 of 23.93 dB and Sa correction of -0.54 dB from 130 on-axis echoes (Table A2.3). This second calibration was also of excellent quality with a RMS deviation of 0.17 dB.

Calibration coefficients estimated from the Campbell Island calibration (which was carried out in similar environmental conditions to those during the survey) was used for the analysis of acoustic data acquired from the Campbell Rise southern blue whiting survey (TAN1905).

Table A2.1. Transceiver settings and other relevant parameters during the calibration.

Parameter	Value
Echosounder	Towbody 4 EK60
EK80 software version	1.12.2
Transducer model	ES38DD
Transducer serial number	28337
EK60 GPT serial number	009072069083
GPT software version	070413
Sphere type/size	tungsten carbide/38.1 mm diameter
Operating frequency (kHz)	38
Towbody depth (m)	3
Transmit power (W)	2000
Pulse length (ms)	1.024
Transducer peak gain (dB)	24.0
Sa correction (dB)	0.0
Sample interval (ms)	0.256
Two-way beam angle (dB)	–20.70
Absorption coefficient (dB/km)	10.0
Speed of sound (m/s)	1500
Angle sensitivity (dB) alongship/athwartship	23.0/23.0
3 dB beamwidth (º) alongship/athwartship	7.0/7.0
Angle offset (º) alongship/athwartship	0.0/0.0

Table A2.2: Auxiliary calibration parameters derived from conductivity, temperature, depth measurements.

Parameter	Campbell Island 17 Sep	Marlborough Sounds 30 Aug
Mean sphere range (m)	19.9	35.3
Mean temperature (ºC)	6.8	12.1
Mean salinity (psu)	34.3	34.7
Sound speed (m/s)	1477	1497
Mean absorption (dB/km)	9.81	9.17
Sphere TS (dB re 1 m^2)	–42.33	–42.41

Table A2.3: Echosounder calibration values for all calibrations of EK60 echosounder in Towbody 4. Transducer peak gain was estimated from mean sphere TS.

Parameter	Campbell Island 17 Sep 2019	Marlborough Sounds 30 Aug 2019	Campbell Island 7 Sep 2016	Campbell Island 6 Sep 2016	Marlborough Sounds 27 Aug 2016
No. of echoes within 0.21° of centre	130	507	290	751	1 302
Transducer peak gain (dB)	23.93	23.88	23.36	23.02	23.54
Sa correction (dB)	-0.54	-0.55	-0.45	-0.51	-0.50
Beamwidth (º) alongship/athwarthship	6.63/6.61	6.95/6.74	7.09/7.09	7.37/7.32	7.22/7.32
Beam offset (º) alongship/athwarthship	0.09/0.07	0.04/0.11	0.00/0.00	-0.00/0.00	0.10/0.09
RMS deviation	0.17	0.16	0.11	0.20	0.05
Echoes used to estimate the beam shape	20 565	12 954	31 555	23 068	14 492

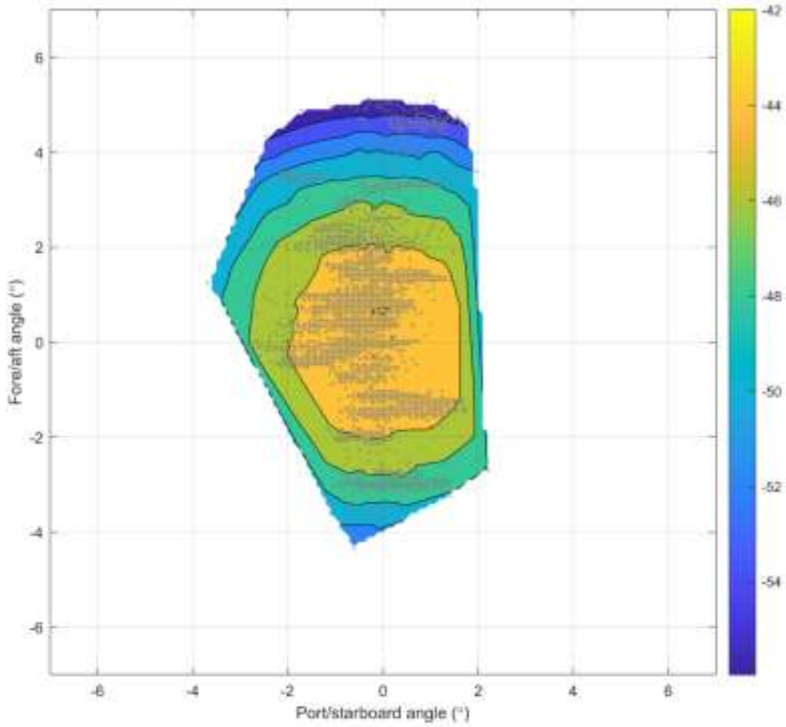

Figure A2.1: The estimated beam pattern from the sphere echo strength and position for the calibration in the Marlborough Sounds. The '+' symbols indicate where sphere echoes were received. The colours indicate the received sphere echo strength in dB re 1 m^2.

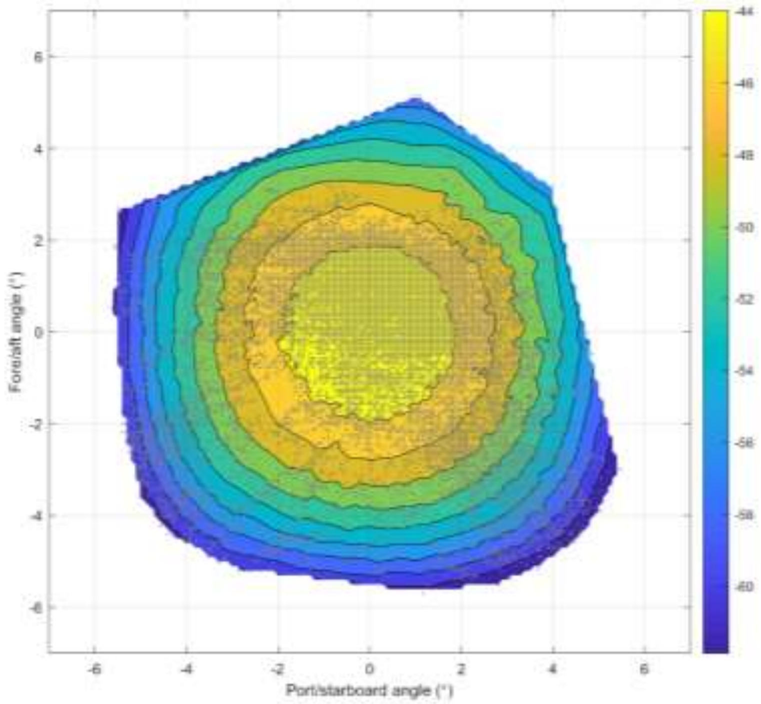

Figure A2.2: The estimated beam pattern from the sphere echo strength and position for the calibration at Campbell Island. The '+' symbols indicate where sphere echoes were received. The colours indicate the received sphere echo strength in dB re 1 m^2.

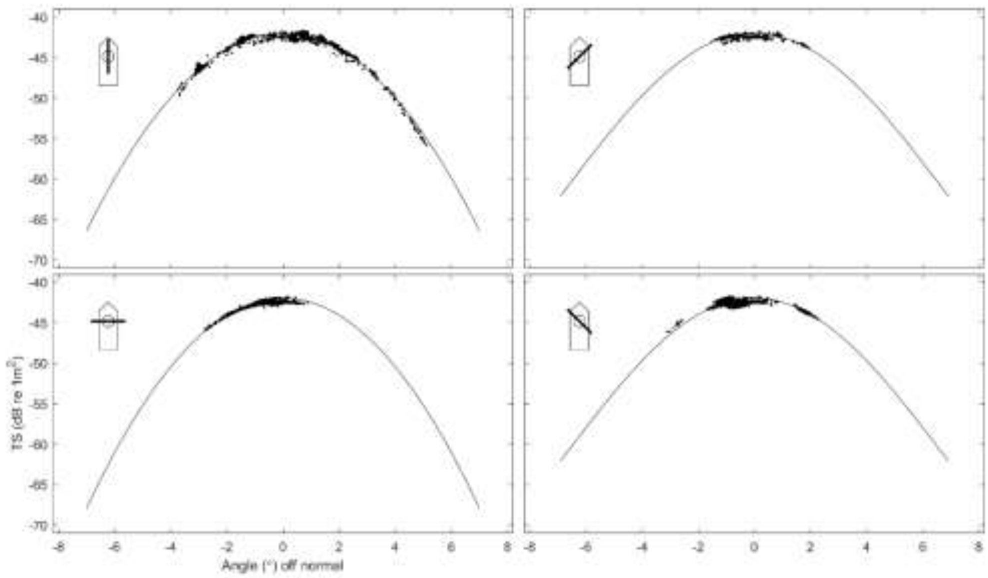

Figure A2.3: Beam pattern results from the calibration analysis for the Marlborough Sounds. The solid line is the theoretical beam pattern fit to the sphere echoes for four slices through the beam.

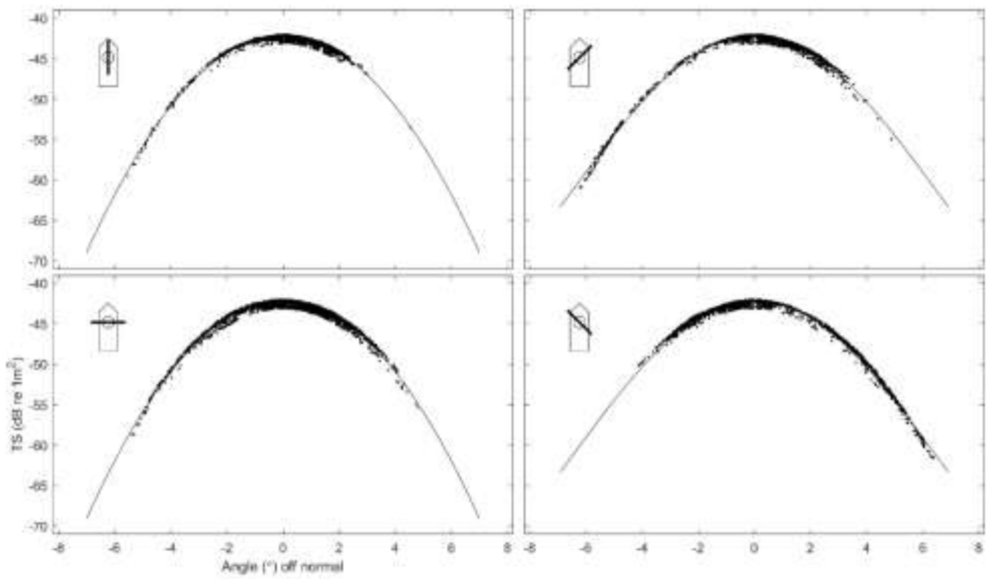

Figure A2.4: Beam pattern results from the calibration analysis for Campbell Island. The solid line is the theoretical beam pattern fit to the sphere echoes for four slices through the beam.

APPENDIX 3: AOS calibration

The dual frequency acoustic optical system (AOS) was calibrated at depth on the probe-deployment (station 18, 19 September 2019), as we attached a 38.1 mm tungsten carbide sphere on a 20 m spectra line.

The methods used for the analysis were similar to those described for the hull transducer and Towbody 4 in Appendix 1 and 2, using ESP3 version 1.7.3. Only the calibration of the 38 kHz system is reported here. Table A3.1 shows the transceiver settings and calibration parameters.

Table A3.2 shows the mean sphere depth and temperature, which was measured concurrently with an RBR duo mounted on the AOS. Because no salinity was measured for this deployment, calculations used a salinity of 34.3 psu, as measured at similar depth from a CTD attached to the net in a previous, nearby trawl (station 17). Corresponding sound speed and absorption used for the calibration data analysis are reported in Table A3.2.

The calibration results are given in Table A3.3. The estimated beam pattern and sphere coverage are given in Figures A3.1 and A3.2. The symmetrical nature of the pattern and the zero centre of the beam pattern indicate that the transducer and WBT tube transceiver were operating correctly. The fits between the theoretical beam pattern and the sphere echoes are shown in Figure A3.3 and confirm that the transducer beam pattern is correct.

The estimated peak gain (G0) of 23.57 dB and the Sa correction of -0.07 dB were estimated from 134 sphere echoes within 0.21° of the beam centre (Table A3.3). This calibration was of excellent quality. The RMS of the difference between the Simrad beam model and the sphere echoes out to 6.8° off axis was 0.18 dB (where <0.2 dB is considered excellent).

Table A3.1. Transceiver settings and other relevant parameters during the calibration.

Parameter	Value
Echosounder	AOS WBT-Tube
EK80 software version	1.12.2
Transducer model	ES38DD
Transducer serial number	28345
WBT-Tube serial number	253685
WBT software version	1.01
Sphere type/size	tungsten carbide/38.1 mm diameter
Operating frequency (kHz)	38
Towbody depth (m)	3
Transmit power (W)	1000
Pulse length (ms)	1.024
Transducer peak gain (dB)	24.0
Sa correction (dB)	0.0
Sample interval (ms)	0.040
Two-way beam angle (dB)	–20.70
Absorption coefficient (dB/km)	10.0
Speed of sound (m/s)	1500
Angle sensitivity (dB) alongship/athwartship	23.0/23.0
3 dB beamwidth (º) alongship/athwartship	7.0/7.0
Angle offset (º) alongship/athwartship	0.0/0.0

Table A3.2: Auxiliary calibration parameters derived from conductivity, temperature, and depth measurements.

Parameter	Station 18 19 Sep
Mean sphere depth (m)	410.0
Mean temperature (ºC)	7.1
Mean salinity (psu)	--
Sound speed (m/s)	1484
Mean absorption (dB/km)	9.33
Sphere TS (dB re 1 m^2)	–42.29

Table A3.3: Echosounder calibration values for the calibration of the 38 kHz echosounder on the AOS. Transducer peak gain was estimated from mean sphere TS.

Parameter	Campbell Island 19 Sep 2019
No. of echoes within 0.21° of centre	134
Transducer peak gain (dB)	23.57
Sa correction (dB)	-0.07
Beamwidth (º) alongship/athwarthship	6.9/6.8
Beam offset (º) alongship/athwarthship	0.03/0.07
RMS deviation	0.18
Echoes used to estimate the beam shape	17 924

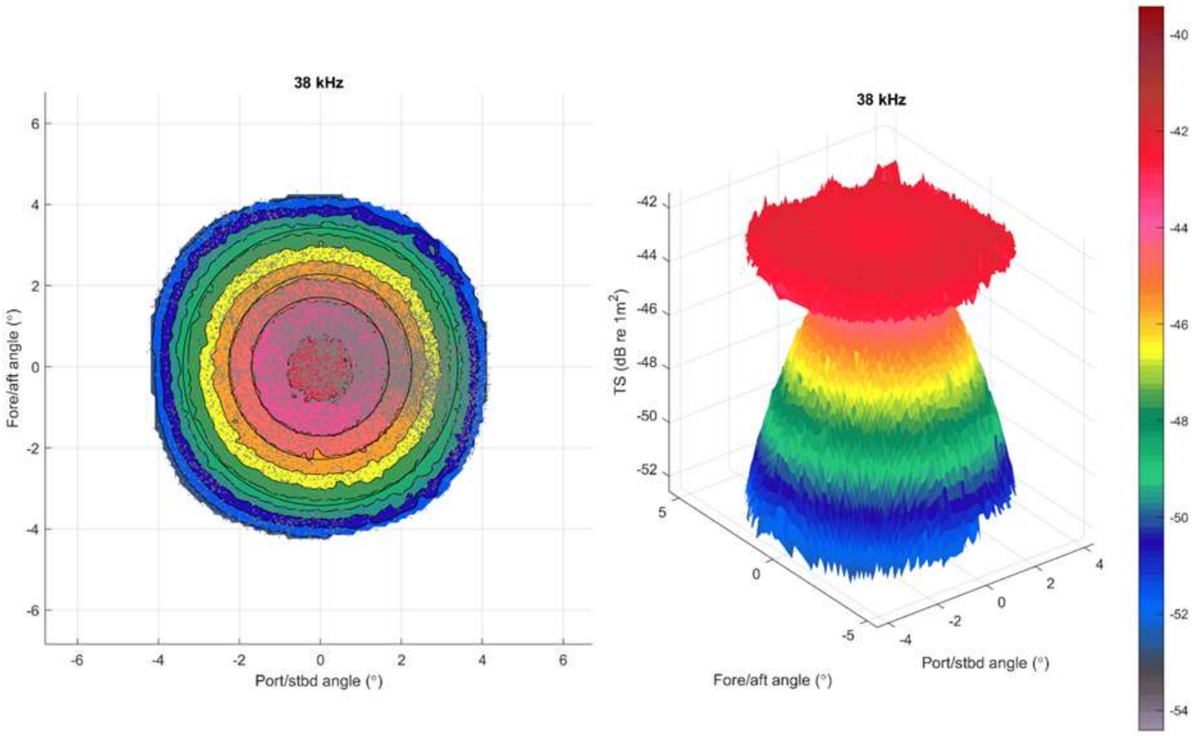

Figure A3.1: The estimated beam pattern of the 38 kHz transducer of the AOS from the sphere echo strength and position for the calibration carried out during station 18 of the 2019 southern blue whiting acoustic survey. The grey dots indicate where sphere echoes were received. The colours indicate the received sphere echo strength in dB re 1 m^2.

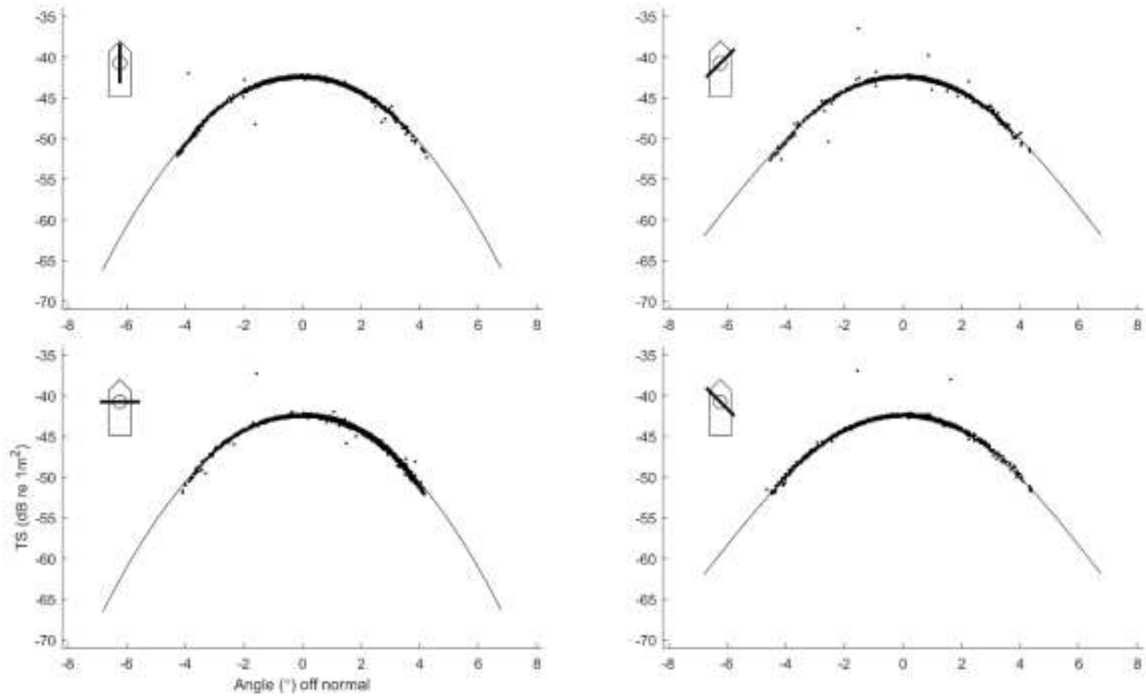

Figure A3.2: Beam pattern results for the calibration of the 38 kHz transducer of the AOS, carried out during station 18 of the 2019 southern blue whiting acoustic survey. The solid line is the theoretical beam pattern fit to the sphere echoes for four slices through the beam.

APPENDIX 4: Description of gonad development used for staging southern blue whiting

Research gonad stage		Males	Females
1	Immature	Testes small and translucent, threadlike or narrow membranes.	Ovaries small and translucent. No developing oocytes.
2	Resting	Testes thin and flabby; white or transparent.	Ovaries are developed, but no developing eggs are visible.
3	Ripening	Testes firm and well developed, but no milt is present.	Ovaries contain visible developing eggs, but no hyaline eggs present.
4	Ripe	Testes large, well developed; milt is present and flows when testis is cut, but not when body is squeezed.	Some or all eggs are hyaline, but eggs are not extruded when body is squeezed.
5	Running-ripe	Testis is large, well formed; milt flows easily under pressure on the body.	Eggs flow freely from the ovary when it is cut or the body is pressed.
6	Partially spent	Testis somewhat flabby and may be slightly bloodshot, but milt still flows freely under pressure on the body.	Ovary partially deflated, often bloodshot. Some hyaline and ovulated eggs present and flowing from a cut ovary or when the body is squeezed.
7	Spent	Testis is flabby and bloodshot. No milt in most of testis, but there may be some remaining near the lumen. Milt not easily expressed even when present.	Ovary bloodshot; ovary wall may appear thick and white. Some residual ovulated eggs may still remain but will not flow when body is squeezed.

APPENDIX 5: Calculation of sound absorption coefficients and sound speed

The Seabird SM-37 Microcat CTD datalogger was mounted on the headline of the net during 16 bottom trawls (including the AOS trawl) to determine the absorption coefficient and speed of sound, and to define water mass characteristics in the area. The water column was unstratified with surface temperatures ranging between 7.0 and 7.5 °C. Average sound absorption was estimated using the formula of Doonan et al. (2003) and the average sound speed using the formula of Fofonoff & Millard (1983) (Table A5.1). The average absorption estimates of 9.41 dB km^{-1} was used to process acoustic data acquired during the 2019 Campbell Island acoustic survey.

Table A5.1: Estimates of acoustic absorption (at 38 kHz) for the Campbell Island Rise acoustic survey area in 2019.

Station	Mean temperature (°C)	Mean salinity (PSU)	Max depth (m)	Absorption (dB/km)	Mean sound speed (m/s)
2	7.42	34.35	316	9.54	1 482
3	7.43	34.36	311	9.47	1 483
4	7.44	34.37	348	9.46	1 483
5	7.47	34.39	429	9.45	1 483
6	7.48	34.39	451	9.40	1 484
7	7.44	34.39	534	9.29	1 485
8	7.44	34.38	425	9.39	1 484
9	7.43	34.39	500	9.35	1 484
10	7.45	34.39	353	9.49	1 483
11	7.45	34.39	400	9.43	1 484
12	7.55	34.41	301	9.47	1 484
13	7.52	34.40	422	9.35	1 485
14	7.64	34.42	516	9.36	1 485
15	7.59	34.42	462	9.38	1 485
16	7.55	34.41	447	9.34	1 485
17	7.44	34.39	416	9.38	1 484
Mean	7.48	34.39	414	9.41	1 484